Effects of Volatile-Char Interactions on Char Structure and Reactivity during the Gasification of Low Rank Fuels

By

Shu Zhang

(B.Eng, M.Chem)

under the supervision of Prof. Chun-Zhu Li

Thesis submitted to MONASH UNIVERSITY for the degree of

Doctor of Philosophy

in the Department of Chemical Engineering

June 2010

Table of Contents

ABSTRACT

Gasification is an efficient thermochemical conversion process to produce syngas that can then be used to generate electricity or to produce liquid fuels and chemicals. Gasification can be applied to many carbon-containing resources: biomass, peat, coal, anthracite, oil residues and municipal solid wastes. Among them, coal (especially brown coal due to its high reactivity) and biomass are the most reliable and abundant feedstocks for gasification.

Advanced gasification technologies are ideal alternatives to the traditional way of fossil fuel utilisation because gasification-based technologies can greatly improve fuel utilization efficiency and meet the increasingly stringent environmental regulations, including CO_2 emission. In the meanwhile, a tailored gasification process for biomass is also highly demanded considering the neutral release of greenhouse gas from biomass utilisation. More importantly, net reduction of CO_2 could be achieved if biomass is utilised in conjunction with a carbon sequestration technology.

Brown coal and biomass have many important unique features compared with the internationally traded black coals. The examples of these features include high contents of moisture, oxygen and aliphatic structure, low contents of aromatic structures, and the presence of well dispersed alkali and alkaline earth metallic species. These structural features and properties make the gasification behaviour of brown coal and biomass distinctly different from that of high-rank coals. Because the volatiles from brown coal and biomass are highly reactive and their chars are unstable, the interactions between volatiles and char can be one of the most important characteristics of brown coal and biomass gasification.

The purpose of this study was to investigate the volatile-char interactions during the pyrolysis and gasification of Victorian brown coal and mallee biomass. Both inter-particle and intra-particle volatile-char interactions were examined in detail. Pyrolysis and gasification experiments were carried out in novel reactors where the extent of volatile-char interactions can be controlled relatively accurately. The structural features of char after various extents of volatile-char interactions were characterised with FT-Raman spectroscopy. The retention of alkali and alkaline earth metallic species in char was also quantified. In addition to the gasification rate of char with steam, the intrinsic reactivity of selected chars in air (O_2) at low temperature was also measured.

The results from this study indicate that the volatile-char interactions could inhibit char conversion during gasification through three possible ways: H radical occupation on reactive sites, changes in char structure and volatilisation of inherent catalysts. Intra- and inter-particle volatile-char interactions were all important for the gasification of char when using large particles. These results indicate that the volatile-char interactions must be considered in the design and operation of gasifiers for Victorian brown coal and biomass.

DECLARATION

I hereby declare that this thesis contains no material which has been accepted for the award of any other degree or diploma at any University or equivalent institution and that, to the best of my knowledge and belief, this thesis contains no material previously published or written by another person, except where due reference is made in the text of the thesis.

Signed:

Date:

ACKNOLOWDEMENT

The period of my PhD study is truly a process of continuous support and imparting knowledge from my supervisor, Prof. Chun-Zhun Li. He guides me not only on the pathway to be an excellent researcher but also on building a correct attitude to life. More importantly, he shows us a wonderful example by his own behaviour all the time. The knowledge and philosophy I learned from him will surely benefit me throughout my life. It will be never enough for me to appreciate such a precious “gift”.

I wish to thank all the group members who ever directly or indirectly gave me support and assistance. My study could not have gone smoothly without their kind and generous cooperation by working in a team. Thanks also go to the administrative officers and technicians in the department for their excellent management and technical help in time.

I am very grateful for the funding from the Victorian state government under its Energy Technology Innovation Strategy program and the funding from the Australian Government as part of the Asia-Pacific Partnership on Clean Development and Climate.

Finally, I would like to express my sincere appreciation to my wife Chen and my daughter Si Rui for their understanding and support. My parents and sisters also encourage me all the time and they have given great help to me in many

ways. Many thanks also go to my parent in–law for their unconditional love and caring on my daughter during my study time.

List of Tables

List of figures

Chapter 1

Chapter 2

Chapter 3

Chapter 4

Chapter 5

Chapter 6

Chapter 1

Introduction

1.1 Background

Energy demand in the world will increase considerably with increasing population and living standard [1, 2]. As is shown in Figure 1-1, the world primary energy demand has continuously increased since 1980, and will be growing at a even higher rate until 2030 according to the International Energy Agency [1]. The share of coal in the global energy demand will climb from 26% in 2006 to 29% in 2030 with the highest growth rate of 2.0 % over the period among the major energy resources [1]. Renewable energy is becoming increasingly important due to the concerns about climate change and energy security although their share is currently very small. Biomass is one of the most important renewable and sustainable energy resources. Biomass could potentially contribute to 10% of the world primary energy consumption by 2030 [1].

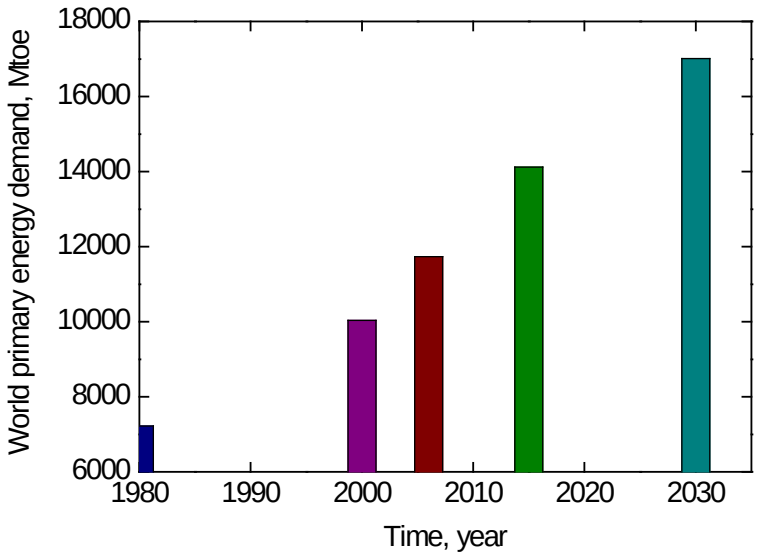

Figure 1-1: World primary energy demand as a function of time [based on the data in Ref 1].

Compared to high rank coals, the majority of low rank coal (e.g. brown coal) is still unexplored due to its low heating value, high moisture content and/or weak coking property. Gasification is widely accepted as a clean thermochemical conversion technology. Biomass and brown coal feature high moisture, high volatile matter yield, high aliphaticity and low aromaticity. Biomass and brown coal are particularly suitable for gasification. During gasification, the volatiles from biomass and brown coal can be very reactive and the corresponding char can be very vulnerable due to their highly aliphatic nature. In a fluidised-bed gasifier, indeed any gasifier, the nascent volatiles will be immediately produced once coal or biomass is fed into the gasifier. Thus, it is inevitable for the volatiles to contact and interact with the vulnerable char. The volatile-char interactions have been recently proved to influence almost every aspect of coal/biomass pyrolysis and gasification [3-7]. Abundant radicals (especially H radicals) could be produced by the thermal cracking and reforming of volatiles. The radicals could adsorb on char surface and penetrate into char matrix, and thus induce changes in char structure and intensify the volatilisation of alkali and alkaline earth metallic (AAEM) species.

More recently, a paper reported that the volatile-char interactions could actually terminate the progress of gasification in steam with the level of char conversion to be achieved depending on the gasification temperature [8]. The inhibition mechanism was simply attributed to the occupation of H radicals on reactive sites of char. However, the reactivity of char could be influenced by many parameters [9-15], in particular, char structure, the concentration and

dispersion of catalysts (mainly AAEM species). The volatile-char interactions could alter these parameters [3-7], and thus potentially contribute to the reduction in char reactivity. Unfortunately, the change in char structure, the retention of AAEM species due to volatile-char interactions and more importantly, how they contribute to the termination of gasification have not been clarified in the previous study [8]. Therefore, there is a need to gain more insights into the mechanism of volatile-char interactions during gasification in steam by conducting experiments under a wide range of conditions.

For biomass, it is well known that the wood chips are very hard to grind into fine particles. The energy consumption is very intensive if biomass has to be ground into very fine particles prior to pyrolysis and gasification. On the other hand, the distribution of biomass particle size always has a wide range due to its fibrous nature, and the difference in particle size could greatly affect heat/mass transfer where biomass is pyrolysed [16-23]. In a biomass gasifier, the primary pyrolysis reactions will generate massive amounts of volatiles inside a particle when its size exceeds a certain level (e.g. > 1 mm). The nascent volatiles will substantially interact with char during their transportation out of the particle. The intra-particle volatile-char interactions may be much more significant and intensive than the inter-particle volatile-char interactions. For the intra-particle volatile-char interactions, the volatiles inside a particle are believed to be more “fresh” and more reactive and also the “fresh” char is more vulnerable. The inter-particle volatile-char interactions are also drastic when a fast heating rate is applied as the pyrolysis is completed in a very short time resulting in high

concentrations of volatile matter inside the gasifier. In contrast, the inter-particle volatile-char interactions are limited at a slow heating rate because the volatiles are produced gradually and thus the volatile concentration inside the particle would be also much lower than at a fast heating rate. There is an essential need to understand the importance of inter-particle and intra-particle volatile-char interactions during the pyrolysis and gasification of biomass. This objective is best achieved by varying the particle size and heating rate experimentally.

Coal sample used in this study is Victorian brown coal. In Latrobe Valley, Victoria, Australia, there is a huge deposit of brown coal which is one of the highest quality brown coal (or lignite) in the world [24]. It was employed as a reliable energy resource (mainly for generating electricity) in Victoria since about one hundred years ago. It will continue to serve as a main energy source for Victorian economy in the foreseen future. Understanding the pyrolysis and gasification behaviour of Victorian brown coal is an important part of the efforts to develop highly efficient gasification technologies for this vast brown coal resource.

Biomass sample used in this study is mallee woody biomass. In Western Australia (WA), about 300 million mallee trees with a short life of regeneration have been planted for dealing with the problem of dryland salinity [25-29]. It was estimated that 10 million dry tonnes of biomass per year [30] could be supplied easily. Gasification will be one of the core technologies for the clean and comprehensive utilisation of this important renewable resource in the future.

The recent studies by this group in Monash and the group in Japan have clearly revealed the importance of volatile-char interactions in the pyrolysis and gasification of low-rank fuels such as brown coal and biomass. The volatile-char interactions affect every aspect of low rank fuel pyrolysis and gasification. Unfortunately, the importance of volatile-char interactions was only discovered by this group recently. Many aspects of volatile-char interactions remain unknown. The main purpose of the study described in this thesis was to investigate the changes in char structure, the changes in AAEM retention and the changes in char reactivity due to volatile-char interactions for two low rank fuels: brown coal and mallee biomass. The study included both inter-particle and intra-particle volatile-char interactions.

1.2 Scope of thesis

Chapter 2 covers experimental details for the subsequent chapters, including the description of key parts of the experimental rig, the experimental procedure/design, and the methods used to characterise char samples.

Chapter 3 to 6 describe the study on the effects of volatile-char interactions on char conversion, char structure and AAEM release during gasification in steam. To begin with, chapter 3 is devoted to the discussion on the effects of volatile-char interactions on char structure during the gasification in steam. Chapter 4 mainly focuses on the explanation of the changes in char reactivity due to volatile-char interactions. This is followed by the exploration of inter- and intra-particle volatile-char interactions during gasification in steam using woody biomass in Chapter 5. Chapter 6 will discuss the drastic changes in char structure upon the introduction of steam using small and large biomass particles respectively.

Chapter 7 will summarize all the study above and make recommendation for the future study in this field.

1.3 References

[1] IEA, World Energy Outlook 2008, International Energy Agency: Paris, 2008.

[2] IEA, World Energy Outlook 2006, International Energy Agency: Paris, 2006.

[3] Li X, Wu H, Hayashi J-i, Li C-Z. Fuel 2004;83:1273.

[4] Wu H, Li X, Hayashi J-i, Chiba T, Li C-Z. Fuel 2005;84:1221.

[5] Quyn DM, Hayashi J-i, Li C-Z. Fuel Process Technol 2005;86:1241.

[6] Wu H, Quyn DM, Li C-Z. Fuel 2002;81:1033.

[7] Quyn DM, Wu H, Hayashi J-i, Li C-Z. Fuel2003;82:587.

[8] Bayarsaikhan B, Sonoyama N, Hosokai S, Shimada T, Hayashi J-i, Li C-Z, Chiba T. Fuel 2006;85:340.

[9] Miura K, Hashimoto K, Silveston PL. Fuel 1989;68:1461.

[10] Mulcahy MFR, Morley WJ, Smith IW. In: Durie RA, editor. The Science of Victorian Brown Coal. Oxford, UK: Butterworth; 1991[chapter 8].

[11] Tomita A, Ohtsuka Y. In: Li C-Z, editor. Advances in the Science of Victorian Brown Coal. Oxford, UK: Elsevier; 2004 [chapter 5].

[12] Takarada T, Tamai Y, Tomita A. Fuel 1985;64:1438.

[13] Lang RJ. Fuel 1986;65:1324.

[14] Takarada T, Nabatame T, Ohtsuka Y, Tomita A. Energy Fuels1987;1:308.

[15] Takarada T, Nabatame T, Ohtsuka Y, Tomita A. Ind Eng Chem Res 1989;28:505.

[16] Anthony D. B, Howard J. B. AIChE J. 1976; 22:625.

[17] Saxena S. C. Prog. Energy Combust. Sci. 1990;16:55-94.

[18] Solomon P. R, Serio M. A, Suuberg E. M. Prog. Energy Combust. Sci. 1992;18:133- 220.

[19] Gavalas G. R, Wilks K. A. AIChE J. 1988;26:201.

[20] Antal M. J. Fuel 1985; 64:1483-1485.

[21] Sonoyama N, Okuno T, Mašek O, Hosokai S, Li C-Z, Hayashi J-i. Energy & Fuels 2006;20:1294.

[22] Kanury A. M. Combust. Sci. Technol. 1994;97:469.

[23] Di Blasi, C. Chem. Eng. Sci. 1996;51:1121.

[24] Li C-Z (editor). Advances in the Science of Victorian Brown Coal 2004; pp1-2.

[25] Wu HW, Fu Q, Giles R, Bartle J. Energy & Fuel 2008;*22:* 190–198.

[26] Wood W. E. J. R. Soc. West 1924;10: 351.

[27] Bartle J, Cooper D, Olsen G, Carslake J. Conserv. Sci. West 2002;4: 96.

[28] Clarke C. J, George R. J, Bell R. W, Hatton T. J. Aust. J. Soil Res. 2002;40: 93.

[29] Cooper D, Olsen G, Bartle J. R. Aust. J. Exp. Agric. 2005;45:1369.

[30] Bartle J. R, Olsen G, Cooper D, Hobbs T. Int. J. Global Energy 2007;27:115.

Chapter 2

Experimental Methods

2.1 Introduction

The general experimental procedures used during the course of this study are detailed in this chapter. In addition to the operational procedures, the feeder and reactor designs, the methods for char characterisation and the preparation of the coal/biomass samples are also detailed in this chapter.

2.2 Experiments in a fluidised-bed/fixed-bed reactor

2.2.1 Preparation of raw sample

For Victorian brown coal, particles between 106 and 150 μm were obtained by sieving the milled coal after drying at a relatively low temperature (<35 °C) [1].

For Australian mallee wood, it was firstly debarked, and then crushed into chips by a pulverizer. The particles between 4.75-5.60 mm were obtained by sieving the crushed wood chips. After drying these particles at 105 °C over-night in nitrogen, the other 8 different particle sizes were directly obtained by crushing the particles of 4.75-5.60 mm in order to minimise the property difference among different particle sizes. The particle sizes used in this study are as follows: 0.90-0.18, 0.18-0.43, 0.43-0.60, 0.60-1.00, 1.00-2.00, 2.00-3.35, 3.35-4.00, 4.00-4.75 and 4.75-5.60 mm.

The properties of the coal and biomass samples are given in Tables 2-1 and 2-2.

Table 2-1. Proximate and ultimate analyses of coal [1] and biomass

Sample	Coal	Biomass
Ash, (wt%, db)	1.1	0.9
Volatile matter (wt%, daf)	52.2	81.6
C , (wt%, daf)	70.4	48.2
H, (wt%, daf)	5.4	6.1
N, (wt%, daf)	0.6	0.2
S, (wt%, daf)	0.3	0.0
Cl, (wt%, daf)	0.1	0.0
O, (by diff.) (wt%, daf)	23.2	45.5

Table 2-2. Contents of AAEM species in coal [1] and biomass.

Sample	Coal	Biomass
Na (wt%, db)	0.10	0.02
K (wt%, db)	0.01	0.07
Mg (wt%, db)	0.06	0.04
Ca (wt%, db)	0.09	0.27

2.2.2 Steam gasification

For the gasification of brown coal at fast heating rates in 15% steam (by volume), a novel fluidised-bed/fixed-bed quartz reactor [1] shown in Figure 2-1 was employed. A two-zone electrical furnace was used to heat up the quartz reactor to the desired reaction temperature (800 °C). In order to achieve a uniform temperature distribution within the reaction zone between the two quartz frits, we fixed the reactor body /reaction zone in the middle of the electrical furnace. By adjusting the temperatures at top and bottom zones of the furnace independently, the temperature difference inside quartz reactor could be controlled well within ± 5 °C (from 795 to 805 °C) when the target temperature is 800 °C.

The configuration of the reactor makes it suitable to investigate the volatile-char interactions. The sand (300-355 μm) bed was fluidised at a total flow rate of 1.8 L/min at room temperature. While the bottom quartz frit acted as gas distributor and fluidising medium supporter, the top frit installed in freeboard would capture all char particles elutriated out of the sand bed. Mixture (1.0 L/min) of argon and steam went into reactor through the fluidising gas tube, as is shown in Figure 2-1. 0.8 L/min of pure argon acting as feeding gas was supplied through the probe where coal particles were fed into the fluidised sand bed. The char particles gradually accumulated underneath the top frit to form a char bed when coal particles were continuously fed into the reactor through the water-cooled probe. At the same time, the volatiles were constantly generated from the devolatilization of coal that was continuously fed into the reactor. The nascent

volatiles must then pass through the char bed in order to get out of the reactor and therefore interact strongly with the char particles. Therefore, the volatile-char interaction time could be easily varied by changing feeding time at a given feeding rate. On the other hand, the concentration of volatiles decreased with decreasing feeding rates of coal (i.e. 100, 50, 30 and 15 mg min^{-1}).

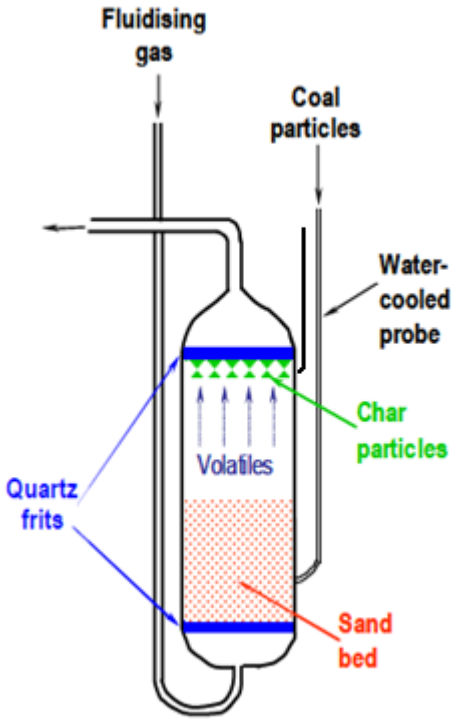

Figure 2-1. A schematic diagram of the modified fluidised-bed/fixed-bed reactor used in this study [1]. Copyright ©2002 Elsevier.

To compare the char conversion in the presence and absence of volatile-char interactions during the gasification in steam, another series of experiments were conducted. After a pre-set feeding period of time, the feeding of coal was suddenly stopped, hence terminating the production of volatiles inside the reactor, However, the supply of steam continued to gasify the char retained underneath the top frit in the absence of volatiles.

The pyrolysis and gasification of biomass at a slow heating rate were carried out in the same type of quartz reactor but without using the water-cooled tube. Instead of feeding through the water-cooled probe, ~5 g of biomass particles were loaded into the reactor through a vertical tube just under the top frit before heating up the reactor to the target temperature at 10 ^{o}C/min. The reactor was held at peak temperature for 15 min before stopping the experiment. 15% steam in argon was supplied by feeding the double-deionized water once the temperature of the reactor reached about 200 ^{o}C. For the experiments aiming to investigate the changes in char structure due to sudden contact with steam at the target temperature, steam (15% by volume) was only introduced to gasify the char after the reactor had reached the desired temperature of (700/800 ^{o}C). The experiments were then terminated by lifting the reactor out of the furnace once the prescribed time of gasification in steam had reached.

The very thin water-cooled probe in the novel fluidised-bed/fixed-bed quartz reactor shown in Figure 2-1 and its corresponding feeding system (see §2.2.3) were unsuitable for large biomass particles. Therefore, the pyrolysis and

gasification of biomass at fast heating rates was conducted in another type of fluidised bed quartz reactor as is shown in Figure 2-2 [2]. The reactor was specially designed for using larger biomass particles. The reactor mainly consists of two parts: the top part is the feeding section and the bottom part is the reaction section. A quartz tube of 14 mm inner diameter was inserted into the reactor through which biomass was fed into the fluidized sand bed. Under the stationary condition, the opening of the feeding tube was just 2 mm above the sand bed. However, during operation it was completely immersed in the fluidized sand bed due to bed expansion on fluidisation. Biomass particles fed through the inner tube were carried with argon gas and were injected into the sand bed. Before feeding, the reactor was heated up to the required temperature. The double-deionised water for steam generation then was introduced through the bottom of the reactor at a concentration of 15% in argon flow. The argon gas flow was reduced and adjusted to maintain the similar fluidisation status of sand particles at different temperatures. When all the parameters were stabilized, the feeding of biomass into the reactor from the feeder was started with the help of an electrical vibrator. About 5.0 g of biomass was fed within 30 min. Then the feeding of biomass and flow of steam were stopped and the reactor was immediately lifted out of the furnace and cooled down naturally with argon flowing through the reactor.

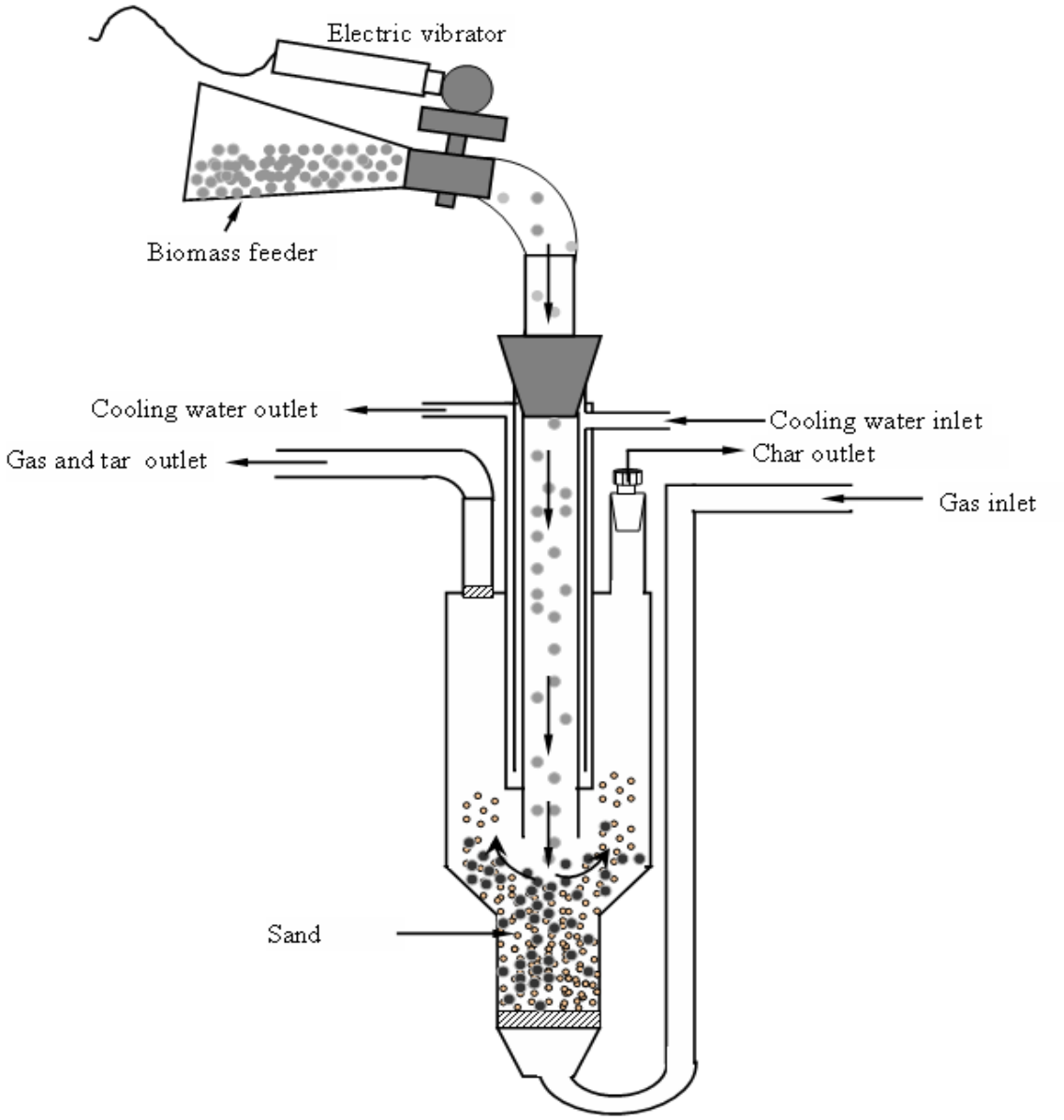

Figure 2-2. A schematic diagram of the fluidised-bed reactor [2] used for investigating the pyrolysis and gasification of large biomass particles at fast heating rates in this study. Copyright © 2009 American Chemical Society.

2.2.3 Feeding system for the fluidised-bed/fixed-bed quartz reactor

Apart from the fluidised-bed/fixed-bed reactor, it is essential to have a reliable, steady and flexible feeder for running experiments. Figure 2-3 shows the schematic diagram of coal/biomass feeding system, which was drawn by Daniel Keown [3].

A round shape glass tube with about 1 cm in diameter and 25 cm in length was used for coal loading. The main reason for selecting glass tube was due to its transparency, so that the feeding status (i.e. the speed and continuity of coal feeding) could be observed. The glass feeder tube was weighed before and after experiments to determine the amount of coal fed into the reactor.

An assembly of two concentric stainless steel tubes was inserted into the free space of the glass feeder (the distance between coal surface and the bottom of the steel tube should be far enough to avoid any possible entry of coal into the reactor before starting feeding). The assembly of two concentric stainless steel tubes and the glass tube were then carefully sealed with the rubber O ring, male and female connections indicated in Figure 2-3. It should be noted that the glass feeder could be still moved up and down when the position of the assembly of two concentric stainless steel tubes was fixed, which allowed the coal inside the glass tube to be close enough to the bottom of the stainless tubes and be blown into the reactor during feeding time. Prior to heating up the reactor, the exit of

feeder was connected with the water-cooled probe in the quartz reactor by using a soft silicon tube. Following the supply of the feeding gas to the outer layer of the concentric steel tube via the T union in Figure 2-3, the fluidising gas from the bottom of reactor was introduced. The sequence should never be forgotten. If the fluidising gas was firstly switched on, the sand could possibly be blown into the water-cooled probe and cause blockage. As shown in Figure 2-3, the feeding gas was going down through outer layer of the steel tube and then going up through inner tube to water-cooled probe in the reactor.

When the reactor was at the target temperature, the coal was fed into the reactor to start the experiments. Now the holding platform supporting the glass tube could be elevated at a controlled speed being controlled by the step motor. The speed will mainly determine the feeding rate of coal sample, which was tested/measured before experiments. The feeding rate was nearly proportional to the speed. The coal could be seen to be entrained into reactor when the distance between coal surface and the bottom of the concentric steel tubes was getting very close (~1 cm). This was the time being considered as the beginning of feeding time. When the prescribed feeding time was reached, we could simply low down the holding platform and then pull down the glass feeder mannualy to terminate the feeding.

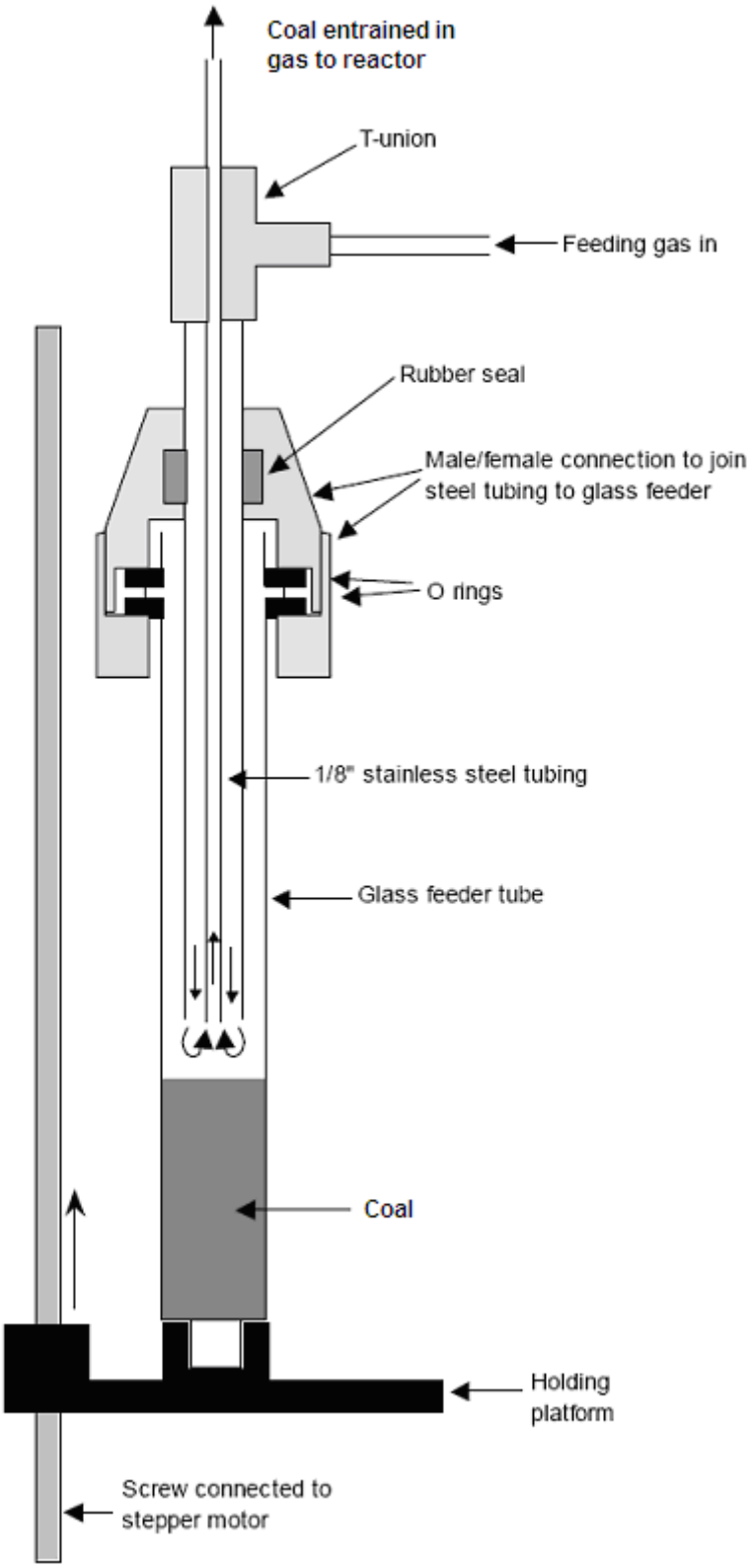

Figure 2-3. A schematic diagram of biomass/coal feeding system [3].

2.2.4 Determination of char yields and collection of chars

The reactor with clean sand filled with air was weighed before each experiment. At the end of an experiment, after the reactor was cooled down naturaly with argon flowing through the reactor, the reactor was taken out of the rig and the tar condensed at the exit of the horizontal tube of the reactor was burned off with a Benson burner under a flow of instrument air. Not only was the air used to blow out the exhausted gas from the combustion of the tar, but to intentionally replace the argon accumulated inside the reactor because the weight of reactor filled with argon could be quite different from that with air. Some water could be possibly condensed due to the steam produced from the combustion of tar. Before taking the weight of the reactor with char, it was held in a 50 °C oven for one hour to dry the surface. About one hour was enough for the reactor to be completely cooled down after taking the reactor out of the oven. The mass difference in the weight of the reactor before and after the experiment was taken as the mass of char. The mass of coal used for the experiment could be easily determined by the mass difference of the glass feeder before and after feeding. But it was also necessary to hold the glass feeder for more than two hours in air to allow the argon inside to diffuse out before weighing it.

After getting the weight of reactor with char, the char was collected for further analysis. To collect char, a cellulous thimber was connected to the tube just underneath the top frit of the reactor, and all the other inlets/outlets were blocked except the fluidising gas inlet. A strong steam of instrument air then flowed through the fluidising tube into the sand-char mixture bed, and exited reactor via

the thimber. Therefore, the char would be elucidated out of the sand bed by the fluidising gas and blown into the thimber while the sand stayed inside. The flow rate of instrument air must be well controlled so that the collected char would not be mixed with sand. The analysed result could be largely affected if there was any sand in the char sample.

2.2.5 Measurement of char reactivity by using TGA

The reactivity of coal char was measured in air at 400°C using a Perkin Elmer Pyris 1 Thermogravimetric Analyser (TGA) following the procedure outlined previously [4]. Briefly, about 4 mg of char sample was placed in a platinum crucible and heated under 99.999% purity of nitrogen atmosphere in the TGA to 105 °C to remove the moisture from the char. The stabilised weight of the char at 105°C was taken as the mass of the dry char. The temperature was then increased at a rate of 50 K min^{-1} to 400 °C. After 2 minutes at 400 °C, the atmosphere was switched from nitrogen to air and reactivity measurement commenced. 400 °C was chosen as the isothermal temperature in this study in order to minimise the changes in char structure due to thermal annealing that would have possibly taken place at higher temperatures. The specific reactivity (R) of the char was calculated using equation:

$$R = -\frac{1}{W}\frac{dW}{dt} \qquad (2\text{-}1)$$

where *W* is the weight (daf basis) of the char at any given time *t*.

After the weight of the char sample had stabilised, the temperature was further increased at 50 K min^{-1} to 600 °C for an additional 30 minutes to ensure

the complete combustion of the carbonaceous material in the char. The mass of ash in the char sample was taken as the final weight after holding for 30 minutes at 600 °C.

The method for the measurement of biomass char reactivity was the same as for coal char outlined above, except that the isothermal temperature of 370 °C was selected rather than 400 °C due to the much higher reactivity of biomass chars. In fact, we tried to use 400 °C initially, but very strong ignition was repeatedly observed for a few samples. 380 °C was then chosen as a second round trial, which also showed the phenomenon of ignition although getting weaker. Eventually, 370 °C was chosen as the proper temperature for the reactivity measurements for all the biomass chars.

2.2.6 Quantification of AAEM in chars

2.2.6.1 Ashing and acid-digestion of char samples

It was shown that the total extraction of the AAEM species was not possible from char unless the char had been ashed to remove the carbonaceous matter [5]. A method was thus developed to remove the carbonaceous matter from coal/char samples without igniting the samples and volatilisation of AAEM [6]. Ignition had to be prevented because the sudden gas expansion that occurs with ignition could cause some of the ash to be blown out of the sample holder.

The char sample was placed in a platinum crucible and ashed in a pure oxygen atmosphere. The oxygen could bond with AAEM and form carbonates in a thermogravimetric analyser (TGA). This further guarantees the zero loss of

AAEM. The temperature was gradually raised at a very slow heating rate to prevent the ignition of the char, and kept for 80 min at 600°C to ensure that only ash left.

Figure 2-4 shows a typical temperature profile of a sample of biomass/char in the TGA during ashing. The char was heated up to 275 °C at 5 °C/min and held for 10 minutes at this temperature. It was then gradually heated up to 415 °C at 2 °C/min. Ater holding at 415°C for 10 minutes, the temperature was further increased to the final temperature of 600 °C at 10 °C/min with 80 min holding time. The reason for the very low heating rate (2 °C/min) between 275 and 415 °C was that the most of the volatiles was produced at this stage. The volatiles were very reactive and would easily ignite if heating rate was high. The use of pure oxygen, the slow heating rate, isothermal periods, relatively low peak temperature and long holding time at the peak temperature together can ensure that no AAEM would be lost while all carbon was fully burnt off.

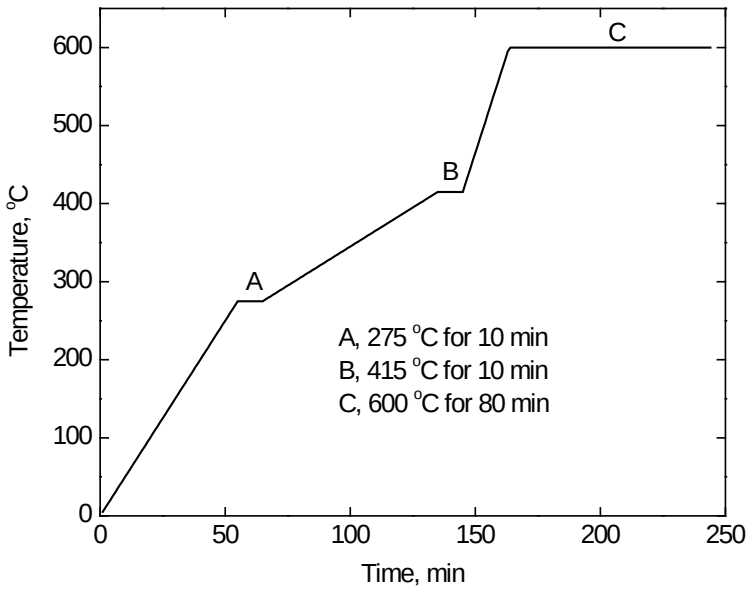

Figure 2-4. A typical temperature profile used in the TGA for ashing chars.

The platinum crucible containing the residual ash was cooled to room temperature and placed into a Teflon vial that already contained 2 ml of concentrated HNO_3 that could wet the ash to prevent the ash from accidentally "flying out". After a batch of char samples had been ashed in this meathod, 2 ml of concentrated HF was added to each Teflon vial containing the ash/HNO_3. The Teflon vials were then sealed and placed on a hotplate. The thermostat on the hotplate was set to a temperature of ~100 °C for a period of no less than16 hours. After the vials were cooled naturally, the lids on the vials were removed and placed (facing up) on the hotplate. The acid in the vials and lids was allowed to evaporate by warming the vials and lids on the hotplate over a period of 4-5 hours. Approximately 10-15 ml of 20 mM methane sulfonic acid (MSA) was then added to each dry vial containing the acid-digested ash. The closed vials containing the MSA solution were firstly shaken to dissolve any AAEM species on the lid, and then warmed for about 10 hours at 50 °C. After cooling to room temperature, the solutions were ready for analysis by ion chromatography.

2.2.6.2 Ion chromatographic techniques

A Dionex DX-500 ion chromatography system was used for this study and it consisted of a GP40 gradient pump and an ED40 electrochemical detector. For all analyses, the pump was operated in the isocratic mode and the detector was operated in the conductivity mode. The principle of using conductivity for ion detection is based on the Kohlraush Law, stating that each ion carries its portion of the total conductivity without being affected by any of the other ions in the solution. The ion exchange columns used in this study were chosen to give good

resolutions for the ions of interest. A guard column was always used to filter out any possible contaminant. Self regenerating suppressors were also used downstream of the ion-exchange columns to improve the intensity of target species.

Quantification of cations

Cation detection was conducted using a CS12A column with a CG12A guard column. A cation self-regenerating suppressor (CSRS-UltraII) was used downstream of the analytical column. The eluent used was 20 mM MSA.

A six-cation standard solution made by Dionex was used for calibrating the response of the detector before the solutions from the acid-digested char/ash samples were run. The six cations were: Li^+, Na^+, NH_4^+, K^+, Mg^{2+} and Ca^{2+} (in that eluting order). The six-cation solution was diluted using 0.2 mM MSA into 6 standard solutions of differing concentrations (covering the expected range of concentrations for unknown samples). The output of the ion chromatography was then converted to a concentration measured in parts per million (ppm). The concentration of cation X in a char sample could then be calculated by knowing the mass of MSA in each sample as well as the mass of the char sample that was ashed (on a dry basis). This calculation is shown as Equation (2-2).

$$[X]_{char\ sample} = [X]_{ppm} \times \frac{Mass_{MSA\ sample}}{Mass_{char\ sample}} \quad (2\text{-}2)$$

The retention of each cationic species in the char was calculated by comparison of its amounts in the raw coal or biomass and the char. The equation used for calculating retention is shown below as Equation (2-3).

$$\%\text{Retention} = \%\text{Char yield} \times \frac{[\text{X}]_{\text{char}}}{[\text{X}]_{\text{biomass /coal}}} \quad (2\text{-}3)$$

2.2.7 Characteristics of char structure by FT-Raman Spectroscopy

The FT-Raman spectra of chars were recorded with a Perkin Elmer Spectrum GX FT-IR/Raman spectrometer following the procedures outlined previously [7-10]. An InGaAs detector constantly cooled in liquid nitrogen was used to collect Raman scattering using a back scattering configuration. The excitation Nd:YAG laser wavelength was 1064 nm. A laser power of 150 mW was used. Each spectrum represents the average of 20 scans. The spectral resolution was 4 cm^{-1}. A curved baseline was considered for each spectrum and the baseline correction was carried out with the software provided by Perkin Elmer with the spectrometer.

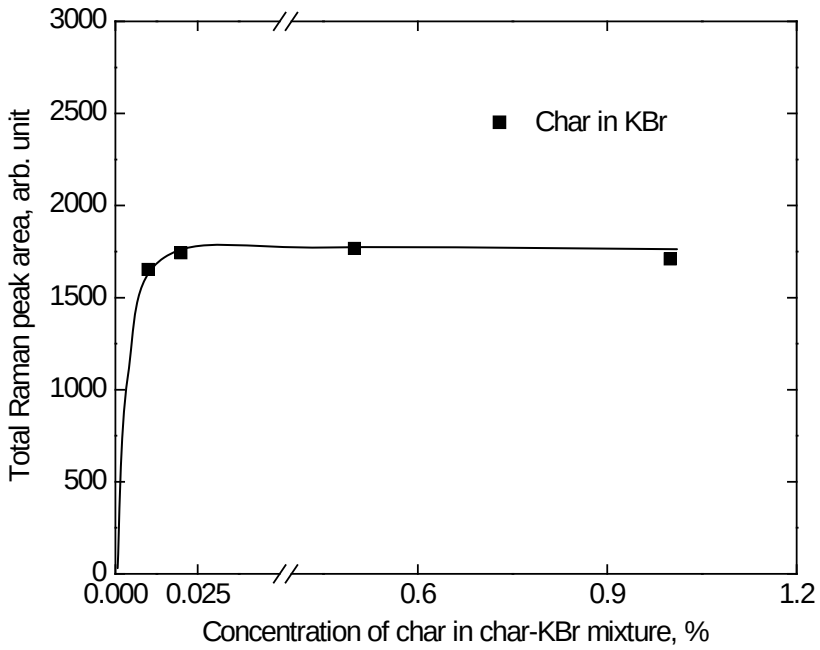

Figure 2-5. Effects of char concentration in the char-KBr mixture on the observed Raman intensity/peak area between 800 cm^{-1} and 1800 cm^{-1} for the char prepared from gasification of brown coal in steam with 50 min feeding time at 100 mg/min at a peak temperature of 800 °C.

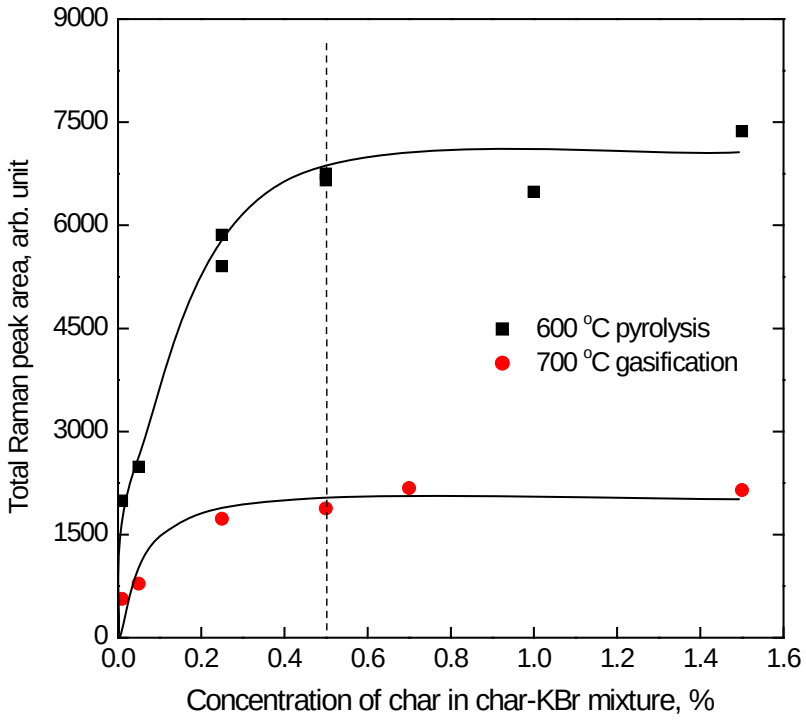

Figure 2-6. Effects of char concentration in the char-KBr mixture on the observed Raman intensity between 800 cm^{-1} and 1800 cm^{-1} for the char prepared from the pyrolysis/ steam gasification of 5.175 mm biomass particles.

Char particles are near black bodies that can be heated up easily in the laser beam, resulting in the emission of Planck radiation [11] and char structural damage. To reduce the heat up of char sample, char was mixed with spectroscopic grade KBr and ground manually. As an excellent heat conductor, KBr helps to avoid sample degradation by allowing the dissipation of heat to prevent the char from being heated up during the acquisition of Raman spectrum.

Figure 2-5 and 2-6 show the effects of char concentration in char/KBr mixture on the observed Raman intensity for char samples prepared from brown coal and biomass respectively. The total peak area between 800 and 1800 cm^{-1} after baseline correction was used as a measure of the Raman intensity. As was the case with previous studies on the Victorian brown coal chars prepared under different experimental conditions [9], the observed Raman intensity approached plateau values at a very low concentration. Therefore, all spectra for coal chars to be reported here were recorded with a char concentration of 0.25 wt% (the same value for the pyrolytic char reported before in our group) in the char-KBr mixture. This concentration was chosen to avoid the complications associated with the heating of char samples by the excitation laser while allowing sufficiently strong signals to be recorded. For the same reason, 0.5 wt% biomass char in KBr was selected for recording spectra for biomass chars, according to Figure 2-6.

As is shown in Figures 2-7 and 2-8, the shapes of the Raman spectra of char, measured as the ratios of peak areas of various Raman bands,

remained unchanged with increasing char concentration for both coal char and biomass chars.

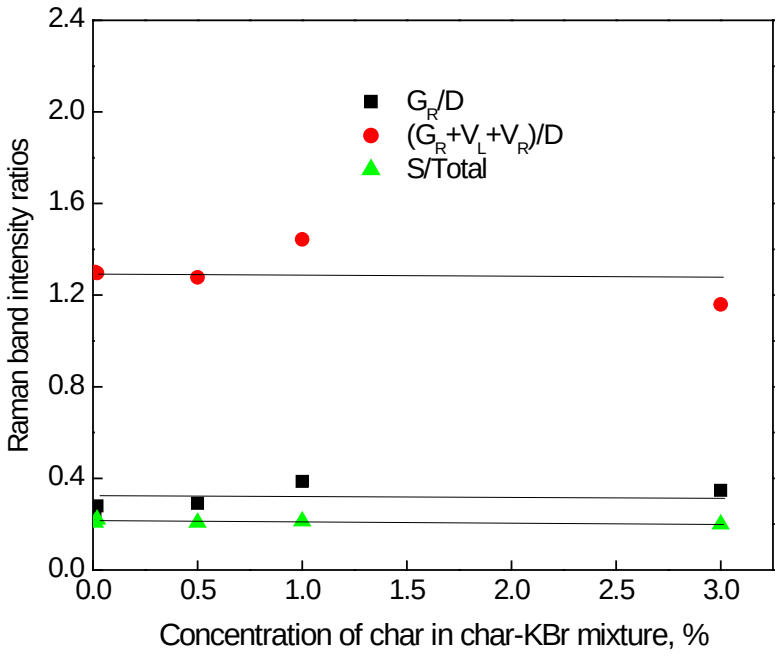

Figure 2-7. Effects of char concentration in the char-KBr mixture on the observed Raman intensity ratios for the char prepared from gasification of brown coal in steam with 50 min feeding time at 100 mg/min at a peak temperature of 800°C.

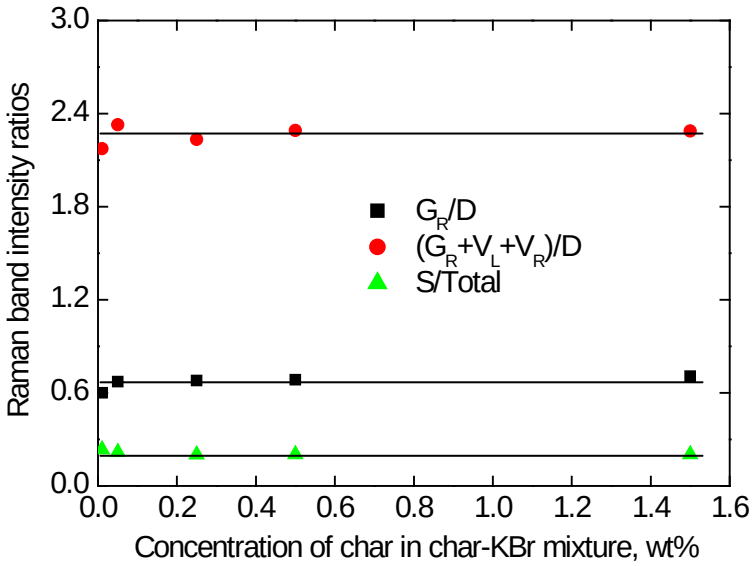

Figure 2-8. Effects of char concentration in the char-KBr mixture on the observed Raman intensity ratios for the char prepared from pyrolysis of 5.175 mm biomass particles at 600 ^{o}C.

The baseline-corrected Raman spectra in the range between 800 and 1800 cm^{-1} were curve-fitted using the GRAMS/32 AI software (version 6.00) with 10 Gaussian bands (Table 2-3) representing the typical structures to be found in chars from low-rank fuels such as brown coal and biomass. A detailed discussion on the band assignment has been reported previously [8]. However, the assignment of the main bands (G, G_R, V_L, V_R, D and S) will be discussed here briefly. The G band at 1590 cm^{-1} mainly represents aromatic ring quadrant breathing and the graphite E_{2g}^2 vibration. The presence of graphite structures was not expected in char, and even if they were, they have been shown to have relatively low Raman intensities [9]. So the observed G band is mainly due to the aromatic ring systems. The D (1300 cm^{-1}) band represents defect structures in the highly ordered carbonaceous materials and, more importantly, aromatics with not less than 6 fused rings. The "overlap" between the D and G bands has been deconvoluted into three bands: G_R (1540 cm^{-1}), V_L (1465 cm^{-1}) and V_R (1380 cm^{-1}). These three bands represent typical structures in amorphous carbon (especially smaller aromatic ring systems) as well as the semi-circle breathing of aromatic rings. The S (1185 cm^{-1}) band mainly represents $C_{aromatic}$-C_{alkyl}, aromatic (aliphatic) ethers, C-C on hydroaromatic rings, hexagonal diamond carbon sp^3 and C-H on aromatic rings.

Figure 2-9 and 2-10 show typical examples of the spectral deconvolution/curve-fitting using the 10 bands; all other Raman spectra in this study showed the similar success of spectral deconvolution.

Table 2-3 A summary of peak/band assignments [8].

Band name	Band position, cm^{-1}	Description	Bond type
G_L	1700	Carbonyl group C=O	sp^2
G	1590	Graphite E^2_{2g}; aromatic ring quadrant breathing; alkene C=C	sp^2
G_R	1540	Aromatics with 3~5 rings; amorphous carbon structures	sp^2
V_L	1465	Methylene or methyl; semi-circle breathing of aromatic rings; amorphous carbon structures	sp^2, sp^3
V_R	1380	Methyl group; semi-circle breathing of aromatic rings; amorphous carbon structures	sp^2, sp^3
D	1300	D band on highly ordered carbonaceous materials; C-C between aromatic rings and aromatics with not less than 6 rings	sp^2
S_L	1230	Aryl-alkyl ether; para-aromatics	sp^2, sp^3
S	1185	$C_{aromatic}$-C_{alkyl}; aromatic (aliphatic) ethers; C-C on hydroaromatic rings; hexagonal diamond carbon sp^3; C-H on aromatic rings	sp^2, sp^3
S_R	1060	C-H on aromatic rings; benzene (ortho-di-substituted) ring	sp^2
R	960~800	C-C on alkanes and cyclic alkanes; C-H on aromatic rings	sp^2, sp^3

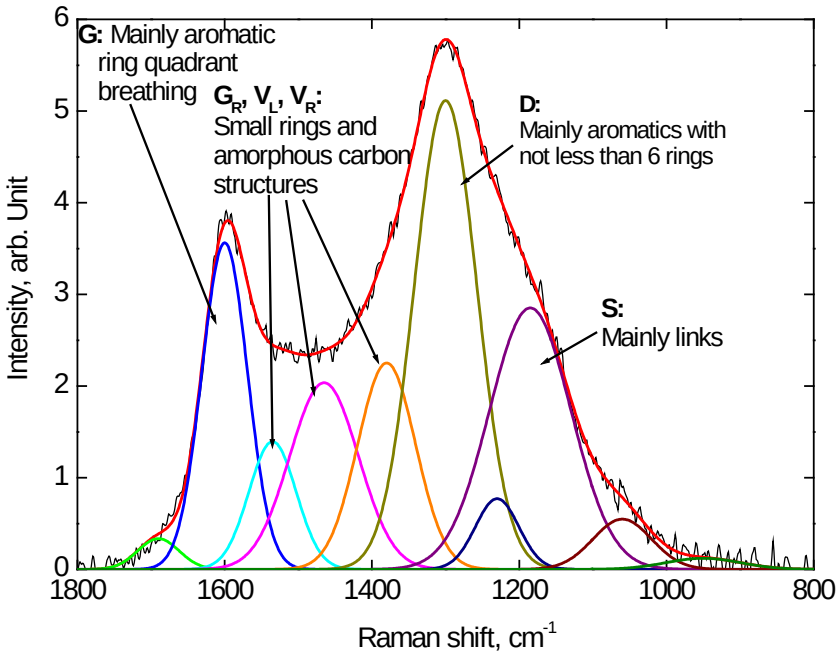

Figure 2-9. Curve-fitting of a Raman spectrum of the char from gasification in steam with 50 min feeding at 100 mg/min at 800 °C.

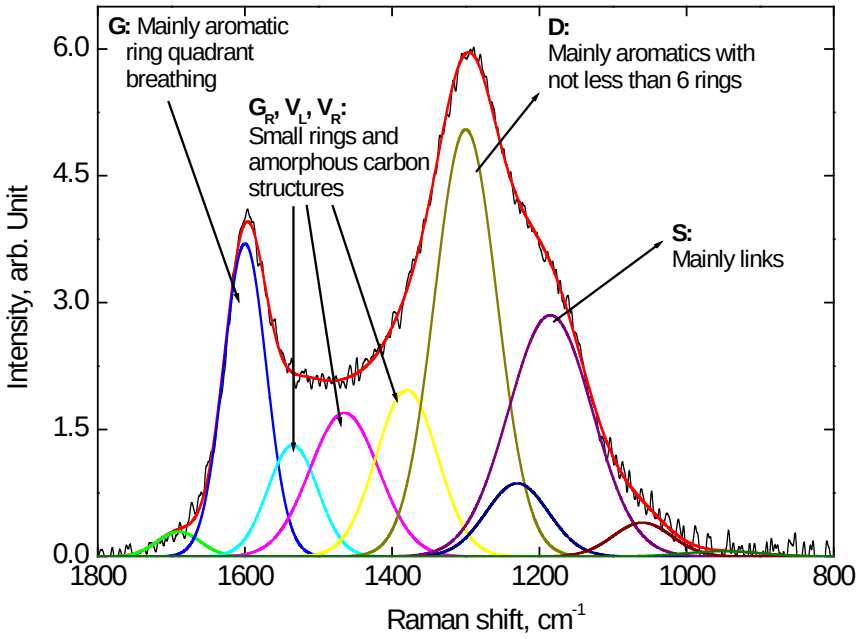

Figure 2-10. A typical example of Raman spectrum fitted with 10 bands. The char was prepared from pyrolysis of the largest biomass particle (5.175 mm) with 15 min holding followed by gasification in steam for 30 min at 800 °C

2.3 References

[1] Quyn DM, Wu H, Li C-Z. Fuel 2002;81:143-149.

[2] Asadullah M, Zhang S, Min ZH, Yimsiri P, Li C-Z. Ind. Eng. Chem. Res. 2009; 48: 9858–9863.

[3] Keown D. Transformation of catalytic species and char structure during the pyrolysis and gasification of biomass (thesis from Monash University), 2007.

[4] Quyn D.M, Wu H, Hayashi J-i, Li C.-Z. Fuel 2003; 82:587-593.

[5] Riley KW, Li C-Z, Kelly MD, Mullins PJ, Nelson PF, Mackay GH. Fuel 1996; 75:780.

[6] Li C.-Z, Sathe C, Kershaw JR, Pang Y. Fuel 2000; 79:427-438.

[7] Li X, Hayashi J-I, Li C-Z. Fuel 2006; 85:1509–1517.

[8] Li X, Li C-Z. Fuel 2006; 85:1518–1525.

[9] Li X, Hayashi J-I, Li C-Z. Fuel 2006; 85: 1700–1707

[10] Li X, Li C.-Z. Ranliao Huaxue Xuebao 2005; 33:385-390.

[11] Quyn D.M, Wu H, Hayashi J-i, Li C-Z. Fuel 2003; 82:587-593.

Chapter 3

Effects of volatile-char interactions on the evolution of char structure during the gasification of Victorian brown coal in steam at 800 °C

Summary

The purpose of this study is to investigate the effects of volatile-char interactions on char structure during gasification in steam. A novel one-stage fluidised-bed/fixed-bed quartz reactor was employed to carry out the experiments in the presence/absence of volatile-char interactions. The structural features of the chars were characterised using FT-Raman spectroscopy.

The results indicate that the char structural features were considerably affected by volatile-char interactions, which was shown from the Raman band area or the ratios between the band areas. H radicals from the thermal cracking/reforming of volatiles are believed to play a vital role in the changes in char structure due to the volatile-char interactions. H radicals could penetrate into char matrix and favour the condensation of aromatic rings, which is the main reason for the decrease in the ratio of small aromatic ring systems to large ones during the volatile-char interactions. The volatile-char interactions also greatly affect the concentrations of O-containing groups in char and thus significantly alter the observed Raman intensity of the char. The presence of O-containing groups in char could dramatically change the observed Raman intensity of the char. The effects of thermal annealing on char structure will be also discussed.

3.1 Introduction

Among various factors influencing the reactivity of char during coal gasification [1-6], the importance of char structure is not particularly well understood. The structure of char ultimately determines the relative ease with which carbon and other atoms of the char are gasified. The structural features of char, e.g. the size of aromatics, the functional groups and the cross-links among them, largely determine the physico-chemical dispersion of catalysts in char [3, 7, 8] and thus greatly influence the activity of the catalysts.

Unlike graphite, the chars from low rank fuels such as brown coal and biomass at relatively low temperatures are composed of a wide range of aromatics and other disordered structures [9, 10]. The structure of these chars can undergo drastic changes during gasification. It is therefore imperative to reveal the evolution of char structure during gasification in order to have a better understanding of the changes in char reactivity during gasification.

Several types of reactions may take place simultaneously to affect the evolution of char structure during gasification. Firstly, the char itself can be thermally decomposed, which has been traditionally termed as the process of “thermal annealing” [11, 12]. Secondly, in agreement with the heterogeneous nature of char structure, certain components/structures of char may be consumed preferentially, resulting in a char structurally different from the original char. It has indeed been shown [1, 2] that smaller aromatic structures (e.g. with 3-5 fused rings) can be preferentially consumed during the gasification of brown coal in air/steam at low temperature. Thirdly, the

reactions of char with gasifying agents may, in addition to the gasification of char itself, bring about changes in the structure of the unreacted portion of the char. In fact, drastic changes in char structure have been observed as soon as the char is exposed to gasifying agents [13].

Many of the reactions responsible for the changes in char structure, e.g. the thermal annealing of char and the reactions between char and gasifying agents, involve radicals (especially hydrogen radicals) [6, 13, 14]. The thermal cracking and reforming of volatiles are an abundant source of radicals. In a commercial fluidised-bed gasifier, volatiles are continuously produced from the decomposition of coal continuously fed into the gasifier at high temperatures. Unavoidably, the nascent and old char stay in an environment filled with volatiles until gasified completely. The interactions between char and volatiles during gasification can generate abundant radicals occupying the char surface. In a moving-bed and entrained-flow gasifier, the volatile-char interactions are also inevitable although could be less significant than those in a fluidised-bed gasifier.

The past work [5, 6, 14-19] in this group has demonstrated that the volatile-char interactions can influence many aspects of the gasification behaviour of brown coal and biomass. During pyrolysis and gasification, the volatile-char interactions could cause drastic volatilisation of alkali and alkaline earth metallic (AAEM) species (especially Na) largely due to the (H) radicals from volatiles [6, 15-18, 20], which would otherwise serve as excellent catalysts for char gasification. The volatile-char interactions could even lead to almost complete termination of char gasification [14]. While experimental

evidence has been obtained to demonstrate the effects of volatile-char interactions on char structure during pyrolysis [5, 6], it remains unclear how volatile-char interactions may affect the evolution of char structure during gasification.

This study aims to investigate the effects of volatile-char interactions on char structure during the gasification of Loy Yang brown coal in steam. The use of a novel fluidised-bed/fixed-bed reactor allowed varying the extent of volatile-char interactions with relative ease. We also attempted to distinguish the effects of volatile-char interactions from those of thermal annealing on the evolution of char structure during gasification.

This study on the changes in char structure is made possible due to the development of a Raman spectroscopic method [4, 5, 9, 21] for the quantification of char structural features, which was used in this study to compare the structural features of char samples prepared under widely different gasification conditions.

3.2 Results and discussion

3.2.1 Effects of volatile-char interactions on char structural features as represented by the ratios of I_{GR}/I_D and $I_{(GR+VL+VR)}/I_D$

I_{GR} is the area of G_R band which originates from the small (3-5 fused rings) aromatic ring systems in char while I_D denotes the area of D band reflecting big (not less than 6 fused rings) aromatic ring systems in char [4, 5, 9, 21]. $I_{(GR+VL+VR)}$ is the total area of (G_R+V_L+V_R) representing amorphous structure including small aromatic ring systems, aliphatics and carboxylates etc [4, 5]. Therefore, the ratios of areas of these bands, I_{GR}/I_D and $I_{(GR+VL+VR)}/I_D$, could reflect the relative ratios between small and big fused rings in chars.

Figure 3-1 shows the ratios I_{GR}/I_D and $I_{(GR+VL+VR)}/I_D$ as a function of coal feeding time during the gasification of Loy Yang brown coal in steam at 800 ^oC. When the coal particles were continuously fed into the reactor at a pre-set constant coal feeding rate, the volatiles were continuously generated to interact with the char. Therefore, the feeding time in Figure 3-1 also means the volatile-char interaction time. Initial rapid drops in both band area ratios with increasing volatile-char interaction time in Figure 3-1 were followed by much slower drops after ~80 min of volatile-char interactions. These results indicate decreases in the ratio of small to large aromatic ring systems with increasing volatile-char interactions time irrespective of feeding rates investigated (15 to 100 mg/min).

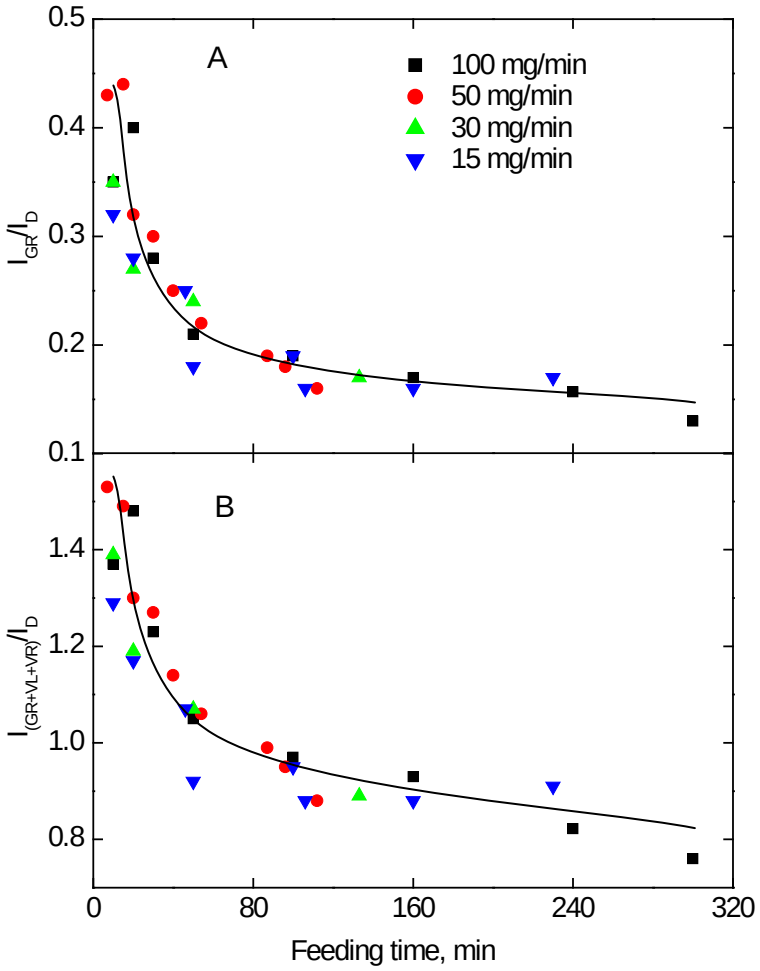

Figure 3-1. I_{GR}/I_D and $I_{(GR+VL+VR)}/I_D$ as a function of feeding time for the chars prepared from the gasification of Loy Yang brown coal in steam with different coal feeding rates.

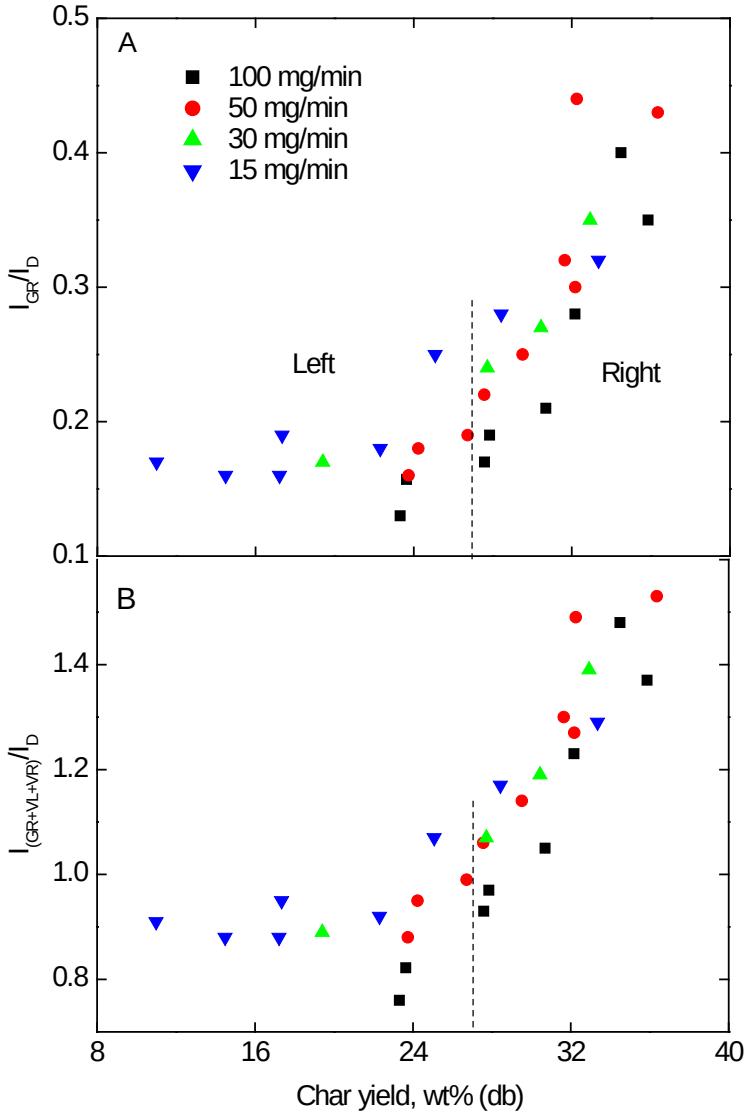

Figure 3-2. I_{GR}/I_D and $I_{(GR+VL+VR)}/I_D$ as a function of char yield for the chars prepared with different feeding time at different feeding rates at 800 °C.

The decreases in the relative abundance of small aromatic ring systems in Figure 3-1 could be due to the preferential consumption of the small aromatics by steam gasification and/or the conversion of the small aromatics into big ones. When the band area ratio I_{GR}/I_D was plotted against the char yield in Figure 3-2, it became clear that the decreases in the relative abundance of small aromatic ring systems, particularly for volatile-char interactions times < ~ 80 min over which the ratios significantly decreased (Figure 3-1), were mainly due to the conversion of smaller aromatic ring systems into bigger ones. On the right part of Figure 3-2, halving the ratio I_{GR}/I_D from ~ 0.45 to ~ 0.22 and the ratio $I_{(GR+VL+VR)}/I_D$ from ~1.5 to ~0.8 took place when the char yield decreased only from ~35 to ~27%.

On the left part of Figure 3-2, the ratios I_{GR}/I_D and $I_{(GR+VL+VR)}/I_D$ had very little change as char yields decreased from ~27% to ~10%, which directly denied the possibility of explaining the data by considering the preferential consumption of small aromatics in the presence of volatiles. As the ratios I_{GR}/I_D and $I_{(GR+VL+VR)}/I_D$ are the properties of the bulk samples, the changes in char structure as reflected by the changes in these ratios must have taken place throughout the char and were not limited on the char surface. The H radicals, due to its mobility and small size, may penetrate into char matrix. The H radicals could firmly adsorb onto aromatic ring systems, even breaking cross-linking structures (e.g. alkyl-aryl C-C) and activate aromatic rings. The activated fused rings could thus loose H radicals and condense into larger

ones. The H radicals from the dehydrogenation of aromatics could continue to activate other aromatic rings or form H_2 released as products.

There appears to exist a limit beyond which volatile-char interactions can no longer effectively change the char structure. At the late stage of feeding time in Figure 3-1(A), the proportion of old char having been interacting with volatiles became larger and larger. The old char structural features were relatively stable/inert and no longer very vulnerable to the active H radicals compared with the nascent char that was formed immediately from the newly-fed coal particles. Therefore, the ratio of I_{GR}/I_D decreased very slowly during a long volatile-char interactions time at the later stage of feeding. Thus, it might be concluded that the ratios I_{GR}/I_D and $I_{(GR+VL+VR)}/I_D$ were mainly dependant on the extent of volatile-char interactions shown in Figure 3-1, and the interactions could transfer the small aromatics into big ones in the presence of abundant H radicals [14, 22, 23], especially at the early stage of feeding time.

The near-zero effect of concentrations of volatiles (feeding rates) on the char structure means that the concentration of volatiles was sufficient for the changes in char structure under the present experimental conditions. In other words, even the H concentration from the feeding rate as low as 15 mg/min could be sufficient to induce the dramatic growth of aromatic rings for the nascent chars.

3.2.2 Volatile-char interactions and thermal annealing

As mentioned in Introduction, the thermal annealing would have also taken place in the process of volatile-char interactions. An attempt was made to investigate the effects of the thermal annealing so that the changes in char structure due to volatile-char interactions and those due to simple thermal annealing during the gasification in steam could be better understood and distinguished. Figure 3-3(A) shows the ratio I_{GR}/I_D of chars as a function of volatile-char interaction time during the gasification in steam and as a function of thermal annealing time (holding in argon) based on 20 min feeding with supply of steam at 800 °C. The ratio I_{GR}/I_D quickly decreased at the beginning in both cases, but then the ratio I_{GR}/I_D for the chars with continuous volatile-char interactions continued to decline slowly whilst the ratio for the char holding in argon stayed nearly constant.

From the comparison of data in Figure 3-3(A), it may seem that the thermal annealing instead of volatile-char interactions was the major factor having caused the significant drop in the ratio of small to large aromatic ring systems owing to the thermal carbonisation/dehydrogenation [24, 25] before ~80 min. However, the char sample prepared from the continuous feeding of coal was always a mixture of old and nascent char. For example, the char from 20 min feeding experiment would consist of the char formed with the coal fed into the reactor at the beginning and the char from the coal particles fed at the last moment of 20 min. The former char experienced 20 min thermal annealing while the latter one was quenched once the coal got into the reactor. Therefore, it should not be forgotten that the average time of thermal annealing for the accumulated chars prepared from continuous feeding was

actually about half of the total feeding time. Therefore, we re-drew the data in Figure 3-3(A) into Figure 3-3(B) in the way that the two trendlines were compared on the basis of the same time of thermal annealing [see Figure 3-3(B)]. The difference between the two trendlines presented in Figure 3-3(B) must be a result of the volatile-char interactions.

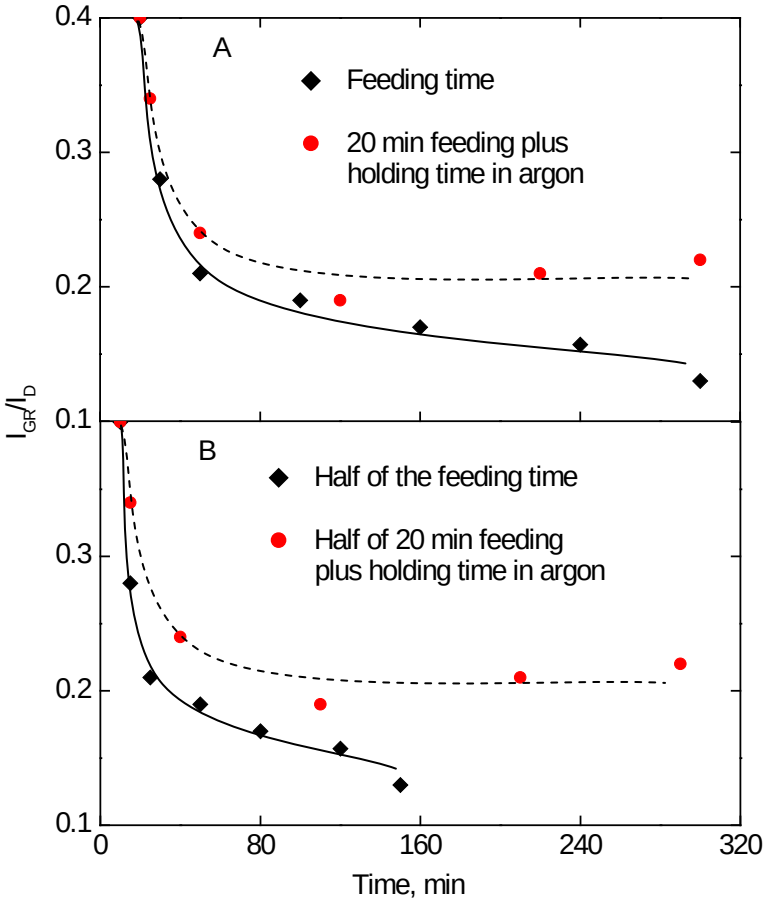

Figure 3-3. A) Ratio I_{GR}/I_D as a function of feeding time at a feeding rate of 100 mg/min and as a function of thermal annealing time following 20 min of coal feeding at 100 mg/min at 800 °C; B) Ratio I_{GR}/I_D as a function of halved feeding time at 100 mg/min feeding rate or as a function of thermal annealing time plus half of 20 min feeding at 100 mg/min at 800 °C.(steam was supplied during feeding time.)

Figure 3-3(B) indicates that the further decrease in the ratio I_{GR}/I_D due to volatile-char interactions could be easily observed. At the early stage of feeding, the ratio I_{GR}/I_D in the case of volatile-char interactions decreased much more significantly than that in the case of thermal annealing alone. At the later stage (after ~80 min), the effects of pure thermal annealing on the ratio became negligible while the volatile-char interactions continued to decrease the I_{GR}/I_D ratio, albeit slowly. Therefore, the volatile-char interactions played a very important role for the changes in char structure.

The essence of thermal annealing of char is the thermal activation of its aromatic ring systems, including the thermal breakdown of substitutional groups on the aromatic ring systems, followed by the growth/condensation of the activated aromatic ring systems. Thermal annealing is therefore a sequence of reactions involving radicals, especially H radicals, and activated aromatic ring systems. The interaction of volatiles with char would bring a lot more (H) radicals to the char surface and across the char matrix through the penetration of H. Those additional H radicals, mainly originating from the cracking and reforming of volatiles, would clearly intensify the reactions of thermal annealing. It is therefore fair to say in the general term that the volatile-char interactions could drastically intensify thermal annealing and that the main reactions involved inside the char are similar for both thermal annealing and the volatile-char interactions.

The features of our fluidised-bed/fixed-bed reactor mean that the majority of char particles would be elutriated out of the sand bed to form a thin bed underneath the top frit through which volatiles and other gases must pass to

exit the reactor. In the thermal annealing experiments, as the char was held for extended periods of time, the products, likely H-rich and even possibly containing H radicals from the thermal decomposition of char particles located at the lower position of the thin char bed, would have to pass through this thin char bed. This effectively provides additional “volatiles” to interact with the char to intensify the ring condensation reactions. Therefore, the data on thermal annealing in Figure 3-3 would somewhat over-estimate the effects of thermal annealing compared with the thermal annealing of “simple/individual” char particles.

3.2.3 Changes in the ratio I_{GR}/I_D due to char-steam reactions in the absence of volatile-char interactions

In order to investigate the change in the ratio I_{GR}/I_D during gasification without volatile-char interactions, feeding of coal was stopped after 55 min of feeding at a feeding rate of 50 mg/min and the char was then held at the same temperature (800 ^{o}C) with the continuous supply of steam. Figure 3-4 shows that the I_{GR}/I_D ratio decreased with decreasing char yield, indicating that the small aromatics were preferentially consumed during gasification in steam in the absence of volatiles, in agreement with our previous study [5, 13].

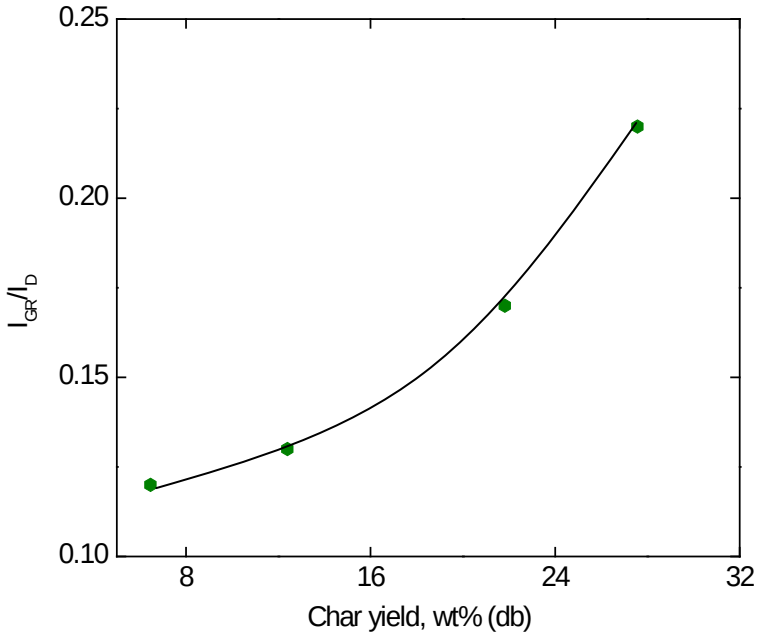

Figure 3-4. The I_{GR}/I_D ratio as a function of char yield for the chars prepared from the gasification of char for varying periods of time after 55 min of coal feeding at 50 mg/min at 800 °C.

3.2.4 Change in the total area I_T during gasification

Raman intensity of char was determined by its Raman scattering ability and its light absorptivity for both excitation laser and Raman scattering [4,5, 9, 21, 26]. The total intensity/area in this study denotes the peak area between 800 to 1800 cm^{-1}. The structural features that could significantly affect the observed Raman intensity are mainly electron-rich elements (i.e. functional groups), the size of fused aromatic rings and the way they bond together. Usually, a high content of O-containing groups in char could result in high Raman intensity via a resonance effect with aromatic rings [27]. The sp^2-rich carbon in big aromatics can theoretically intensify Raman intensity more than sp^3 carbon through conjugation with other sp^2 bonds. However, sp^2-rich carbon also has a stronger light absorptivity than sp^3 carbon [27]. As a result, the increasing aromatic ring size usually results in decreases in the overall intensity due to the dominant role of light absorbing ability [9, 13, 28].

Figure 3-5(A) shows the relationship between the total Raman intensity of chars and the volatile-char interaction time (feeding time). The total intensity of the chars scattered badly though the average of them appeared to be constant. Clearly we could not attribute the change in the total intensity to the change in the ratio of small aromatics to large ones: the ratio in Figure 3-1 showed a very smooth trend. Considering the practical experimental operations for producing the chars, the trend in the total intensity could be likely ascribed to those O/H-containing structures in char. The functional groups in char are unstable although extremely important for the observed Raman intensity. During experiments, the feeding rate may be un-even at short time scales. At the end of coal feeding, the gas atmosphere surrounding

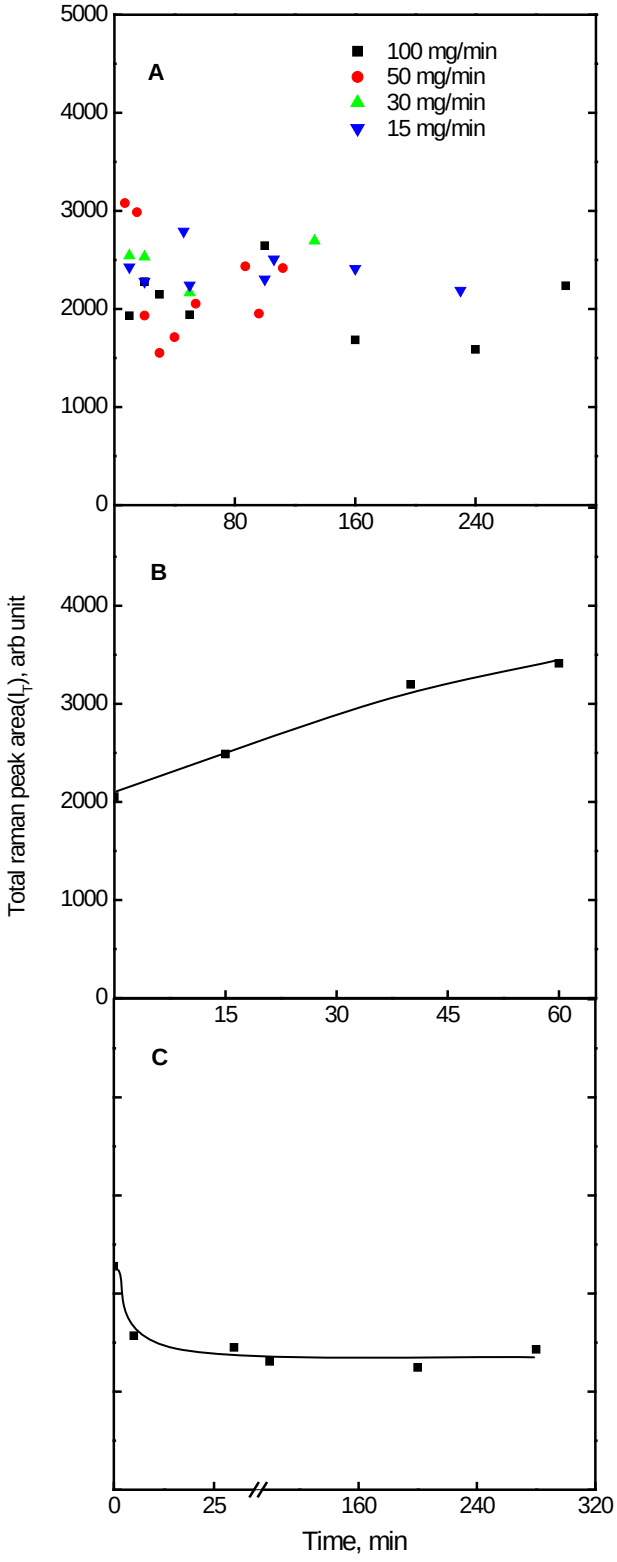

Figure 3-5. The Raman total peak area I_T between 800 and 1800 cm^{-1} as a function of reaction time at 800 °C. A) Chars were prepared from different feeding time in steam at different feeding rates; B) Chars were prepared from different holding time in steam after 55 min feeding at 50 mg/min; C) Chars were prepared from different holding time in argon after 20 min feeding in steam at100 mg/min.

the particles changed as soon as the production of volatiles and supply of steam was stopped. The true holding time at the end of feeding time was not possible to be exactly zero because a short moment was needed to lift the reactor out of the hot furnace. Instead, it could vary for quite a few seconds. If the time was short, some O-containing and H-containing groups that had not been decomposed/gasified would stay in the char. The uncontrollable variation of holding time at the scale of seconds after the end of coal feeding could result in chars containing different amounts/forms of these unstable structures (O-containing and H-containing groups). In this case, the observed Raman peak area could change drastically and lead to non-reproducible total intensity

The contrast between the non-reproducible total intensity (Figrue 3-5(A)) and the relatively repeated Raman peak shape (i.e. the peak area ratios [Figures 3-1 to 3-3)] further confirms that the variation in intensity was mainly due to the varied amounts/forms of O-containing functional groups in char. O-containing functional groups can, through their resonance effects, cause big changes in the observed Raman intensity even when the core aromatic ring systems remained largely unchanged.

For the gasification in the absence of volatile-char interactions, the total intensity increased with gasification, as is shown in Figure 3-5(B). During the reaction of carbon (char) with steam, H_2O would dissociate into O or O-containing radicals on the char surface. While H radicals would combine to form H_2 and desorb from chars, O-containing species could react with char to form various O-containing intermediates (complexes). The oxygen complexes

formed in char as a result of the partial oxidation reaction between char and steam could increase the observed Raman intensity [29].

Figure 3-5(C) shows the total observed Raman intensity of chars versus holding time in argon (i.e. thermal annealing alone). The chars were prepared after different holding time in argon after 20 min feeding with the continuous supply of steam. The total intensity dropped markedly from 2400 to about 1500 within 5 min holding in argon, then kept constant. If considering the phenomena in Figure 3-5 (A), the error could be very big for the first point in Figure 3-5(C) as the true holding time could not be controlled exactly. In other words, the real time taken for the reactor to be moved out of the hot furnace was very crucial to the observed Raman intensity as stated above.

Nevertheless, the unchanged low total intensity after a short period of holding in argon again indicated the importance of the volatiles (formation of O-containing structures on/in char) on the observed Raman total intensity. Once the char had been held in argon for more than seconds or a minute, the relatively unstable O-containing structures formed from the char-steam reactions would have decomposed. This provides a plausible explanation of the smooth trend in Figure 3-5(C), compared with that in Figure 3-5(A).

It must be emphasised that the O-containing structures would mainly act as “sensitisers” to enhance the observed overall Raman intensity. These O-containing structures have little effects on the Raman peak shape (i.e. the ratios I_{GR}/I_D, $I_{(GR+VL+VR)}/I_D$ shown in Figures 3-1 to 3-3).

3.2.5 Change of ratio I_S/I_T during the gasification

Theoretically, S band mainly represents alkyl–aryl C–C structures, aromatic (aliphatic) ethers and C-C in hydroaromatic rings in char [5, 30, 31]. Typically, the S band can be considered as a brief measure of cross-link structures in a char. The ratio I_S/I_T was examined for all the chars above. Being consistent with the previous study [5], all the chars from different experimental conditions showed nearly the same value of I_S/I_T in Figure 3-6, which indicates that the cross-link structures represented by the S band could not be selectively consumed by steam gasification regardless of the presence of the volatiles, even the pyrolysis in argon. Basically the unstable carbon structure must have been thermally cracked down during primary decomposition once the coal was fed into the fluidised-bed reactor at the temperature. The cross-link structures then remaining in char was very stable, so that they cannot be preferentially consumed under the experimental conditions examined. The chars experienced the same primary decomposition process thus the relative ratio of I_S/I_T could keep almost constant, as is shown in Figure 3-6.

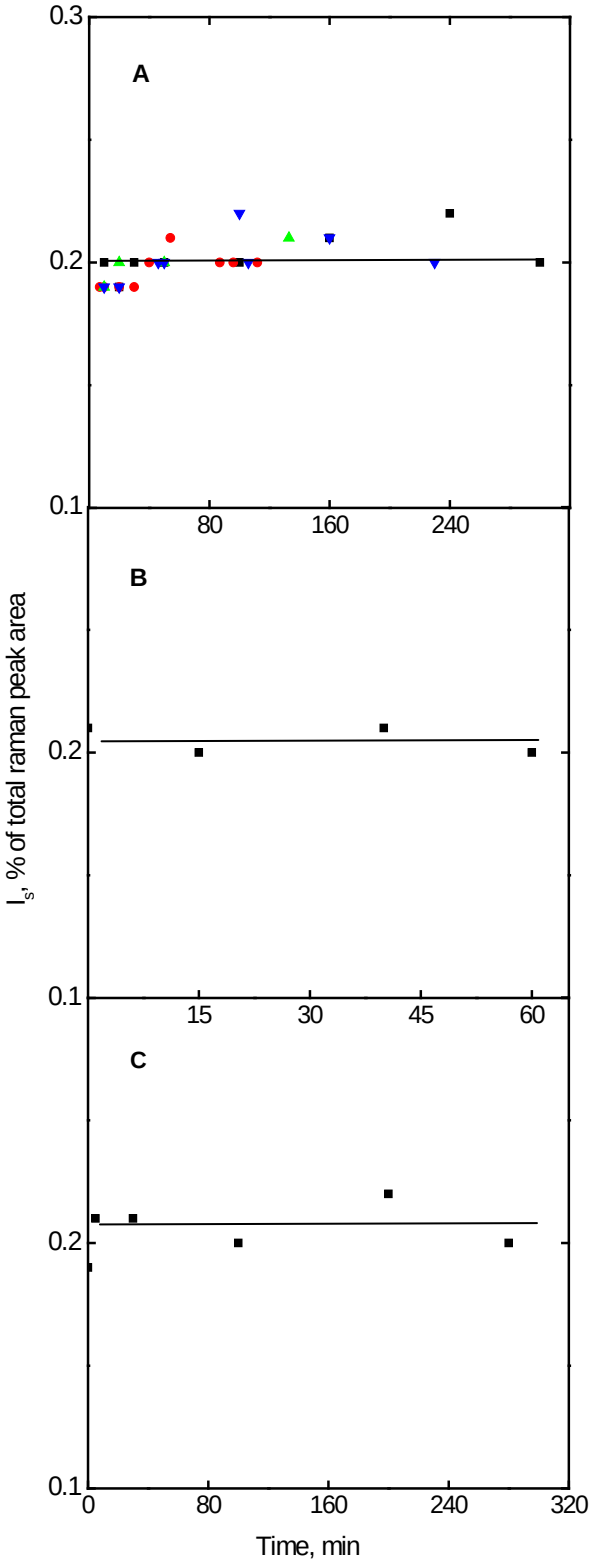

Figure 3-6. Ratio I_S/I_T as a function of reaction time at 800 °C. A) Chars were prepared from different feeding time at different feeding rates in steam; B) Chars were prepared from different holding time in steam after 55 min feeding at 50 mg/min; C) Chars were prepared from different holding time in argon after 20 min feeding in steam at100 mg/min.

3.3 Conclusions

The effects of volatile-char interactions on the evolution of char structure during the gasification of Victorian brown coal in steam have been studied in a fluidised-bed/fixed-bed quartz reactor. The extents of volatile-char interactions were controlled by varying the coal feeding time and/or coal feeding rate. The structural features of chars have been characterised with FT-Raman spectroscopy. Volatile-char interactions greatly enhanced the conversion of small aromatic ring systems into big ones during the gasification in steam. The volatile-char interactions and the thermal annealing appear to have great similarities in terms of activation and condensation of aromatic ring systems. H radicals are believed to play important roles during volatile-char interactions. The results imply that H radicals mush have penetrated deep into the char matrix to induce the condensation of aromatic ring systems. The evolution of char structure during gasification in the absence of volatile-char interactions showed very different characteristics from that in the presence of volatile-char interactions. Volatile-char interactions also appear to have strong influence on the presence of O-containing functional groups in char. These O-containing structures can decompose readily as soon as the volatile-char interactions ceased. Additionally, O-containing functional groups from volatiles were very critical for the observed Raman total intensity of chars. However, the relative ratio of cross-link structure represented by S band in the chars was almost same for the experimental conditions used.

3.4 References

[1] Miura K, Hashimoto K, Silveston P. L. Fuel 1989; 68:1461-1475.

[2] Li X, Wu H, Hayashi J-I, Li C-Z. Fuel 2004;83: 1273–1279.

[3] Wu H, Li X, Hayashi J-i, Chiba T, Li C-Z. Fuel 2005;84:1221-1228.

[4] Li X, Hayashi J-I, Li C-Z. Fuel 2006;85:1509–1517.

[5] Li X, Li C-Z. Fuel 2006;85:1518–1525.

[6] Li C-Z. Fuel 2007;86:1664–1683.

[7] Quyn DM, Wu H, Hayashi J-I, Li C-Z. Fuel 2003;82:587–593.

[8] Takarada T, Tamai Y, Tomita A. Fuel 1985;64:1438-1442.

[9] Li X, Hayashi J-I, Li C-Z. Fuel 2006;85: 1700–1707

[10] Hayashi J-i, Li C-Z. Structure and properties of Victorian brown coal. In: Li C-Z, editor. Advances in the science of Victorian brown coal. Oxford: Elsevier; 2004. p. 11–84 [chapter 2].

[11] Zolin A, JensenA, Dam-Johansen K, Jensen L-S. Fuel 2001; 80:1029-1032.

[12] Sennbca O, Russo P, Salatino P, Masi S. Carbon 1997; 35,:141-151.

[13] Keown D. M, Hayashi J.-I, Li, C.-Z. Fuel 2008;87:1127-1132.

[14] Bayarsaikhan B, Sonoyama N, Hosokai S, Shimada T, Hayashi J-i, Li C-Z, et al. Fuel 2006;85:340-349.

[15] Quyn DM, Wu H, Li C-Z. Fuel 2002;81:143-149.

[16] Quyn DM, Wu H, Bhattacharya SP, Li C-Z. Fuel 2002;81:151-158.

[17] Wu H, Quyn DM, Li C-Z. Fuel 2002;81:1033-1039.

[18] Sathe C, Hayashi J-I, Li C-Z, Chiba T. Fuel 2003;82:1491-1497.

[19] Quyn DM, Hayashi J-i, Li C-Z. Fuel Process Technol 2005;86:1241.

[20] Keown D. M, Hayashi J.-I, Li, C.-Z. Fuel 2008;87:1187-1194.

[21] Li X, Li C.-Z. Ranliao Huaxue Xuebao 2005;33:385-390.

[22] Juntgen H. Carbon 1981;19:167–173.

[23] Huttinger KJ, Merdes WF. Carbon 1992;30:883–894.

[24] Morgan J-J, Soule R-P. Chemical and Metallurgical Engineering 1922; 26:1025-1030.

[25] Berkowitz N, Den H-W. Fuel 1962; 41:507-520.

[26] McCreery RL. Raman spectroscopy for chemical analysis. New York:Wiley–Interscience; 2000.

[27] Leites LA, Bukalov, SS. J. Raman Spectrosc. 2001; 32:413-424.

[28] Keown D. M, Li X, Hayashi J-I, Li C-Z. Energy & Fuels.2007;21:1816-1821.

[29] Guo X, Tay HL, Zhang S, Li C.-Z. Energy & Fuels. 2008; 22: 4034-4038.

[30] Schwan J, Ulrich S, Batori V, Ehrhardt H. J Appl Phys 1996;80:440–447.

[31] Nemanich RJ, Glass JT, Lucovsky G, Shroder RE. J Vac Sci Technol A 1988;6:1783–87.

Chapter 4

Effects of volatile-char interactions on char-H_2O and char-O_2 reactivities

Abstract

Recent studies have shown that the volatile-char interactions are an important consideration in the design and operation of a gasifier. This study aims to investigate the effects of volatile-char interactions on the *in situ* char-steam reactivity at 800°C and the *ex situ* char-O_2 reactivity at 400°C. A Victorian brown coal was gasified in 15% steam at 800°C in a one-stage novel fluidised-bed/fixed-bed quartz reactor, in which the extents of volatile-char interactions could be controlled. The chars after varying extents of volatile-char interactions and/or varying extents of char conversion in steam were also collected for the measurement of their reactivity with air at 400 °C in a thermogravimetric analyser. Our results show that the char-steam gasification reactions were greatly inhibited by the volatile-char interactions. It is believed that the H radicals generated from the thermal cracking/reforming of volatiles slowed the char gasification in three ways: occupying the char reactive sites, causing the char structure to re-arrange/condense and enhancing the release of catalytic species inherently present in the brown coal. The importance of volatile-char interactions to char-steam reactivity was further confirmed by the char-air reactivity. However, our results indicate that the char-steam and char-oxygen reactions probably follow different reaction pathways.

4.1 Introduction

The need to operate gasification at high temperature and pressure contributes significantly to the limited gasification efficiency and high capital/operating costs. This can be dramatically improved by developing the second generation coal gasification technologies where coal is gasified at low temperatures. High char reactivity is essential to realising the full potential of a low-temperature gasification process. Therefore, intensive research has been performed to investigate the factors affecting char reactivity. Three key factors influencing char reactivity are the presence of catalysts in char [1-12], the structural features of char itself and the interactions between catalysts and char [10, 13-19].

Volatiles interact strongly with char in practical gasifiers, particularly in fluidised-bed gasifiers. Volatile-char interactions have been experimentally proved to be a crucial factor during the pyrolysis of brown coal, which favours the release of alkali and alkaline earth metallic (AAEM) species, activates the growth of aromatic rings and reduces the (ex-situ) char reactivity [3, 19-22]. Therefore, such problems as the erosion of turbine blades by the volatilised AAEM species and the low char reactivity in a gasifier are closely related with the extent of volatile-char interactions. In the worst case [18], increases in the gasification temperature for a brown coal do not necessarily lead to increases in the char reactivity. Further detailed investigation on the reactions responsible for the observed effects of volatile-char interactions under gasification condition is warranted.

In particular, the effects of volatile-char interactions on the in situ char reactivity during gasification in steam at elevated temperature remain poorly understood. Our recent paper [23] reported that the interactions of volatiles and char could practically terminate the char conversion with the exact char conversion level at which gasification stops depends on gasification temperatures. H radicals originated from the thermal cracking/reforming of volatiles were believed to be responsible for the inhibition of the gasification reactions by occupying the reactive sites of char surface.

Although our previous work [23] has demonstrated the importance of volatile-char interactions on char conversion, the exact roles of H radicals require further clarification. Except from occupying reactive sites on char surface, H radicals could also change char structure and AAEM retention/dispersion in char; both would alter char reactivity. There is a need to appreciate the individual roles of each factor, viz. the adsorption of H radical on char surface, the change in the char structure and the catalyst concentration/dispersion, in determining the char reactivity. The ability to control the extent of volatile-char interactions is essential in appreciating the roles of each above-mentioned factor in influencing the char reactivity.

Continuing our recent efforts to study the volatile-char interactions [15-18], this study aims to examine the effects of volatile-char interactions on the *in situ* char reactivity during the gasification in steam and on the *ex-situ* char reactivity in air after the gasification in steam. The extent of volatile-char interactions was controlled by adjusting the volatile-char interaction time and the concentration of volatiles (H radicals) interacting with char independently.

Moreover, the char reactivity data are correlated with the changes in char structure and the concentration of catalysts inherently present in brown coal. Our results also provide additional insights into the difference in the reaction pathways between the char-steam at 800°C and char-O_2 at 400°C.

4.2 Results and discussion

4.2.1 Char conversion during gasification in steam in the presence of volatile-char interactions

Figure 4-1 shows the conversion of coal during the gasification in steam as a function of feeding time (volatile-char interaction time) at feeding rates ranging from 15 to 100 mg/min. After a fast char conversion before ~80 min feeding, the gasification of coal slowed down, especially at high feeding rates, even in the presence of steam. Particularly, the highest feeding fate of 100 mg/min used in this study has led to a very limited coal conversion at the later stage of feeding time.

At the early stage of feeding time, the proportion of nascent char was relatively large. Therefore, the char conversion rate was high at the early stage of feeding as the nascent char featured high reactivity.

However, with the progress of the gasification/feeding, the average age of chars increased, becoming less reactive due to the large proportion of big aromatic ring systems shown in Figure 3-1. With increasing feeding time, the char accumulated underneath the top frit to form an increasingly thick char bed. The increasing thickness of char bed extended the interacting time with

volatiles when they passed through. More H radicals from the thermal cracking/reforming of volatiles could be produced from the longer period of volatile-char interactions, which is supported by the following evidence. During the experiments, a bubbler containing 0.02 M MSA solution was connected to the exit of the reactor. We changed the bubbler every 20 min while the coal particles were continuously fed. The first two bubblers were quite yellowish although the second one was much lighter. Surprisingly, starting from the third one, the bubbler was always colourless and the tar collected, if any, was not observable. This phenomenon indicates that the large aromatic ring systems in tar were reformed/cracked into light gases and small hydrocarbons due to the intensified volatile-char interactions.

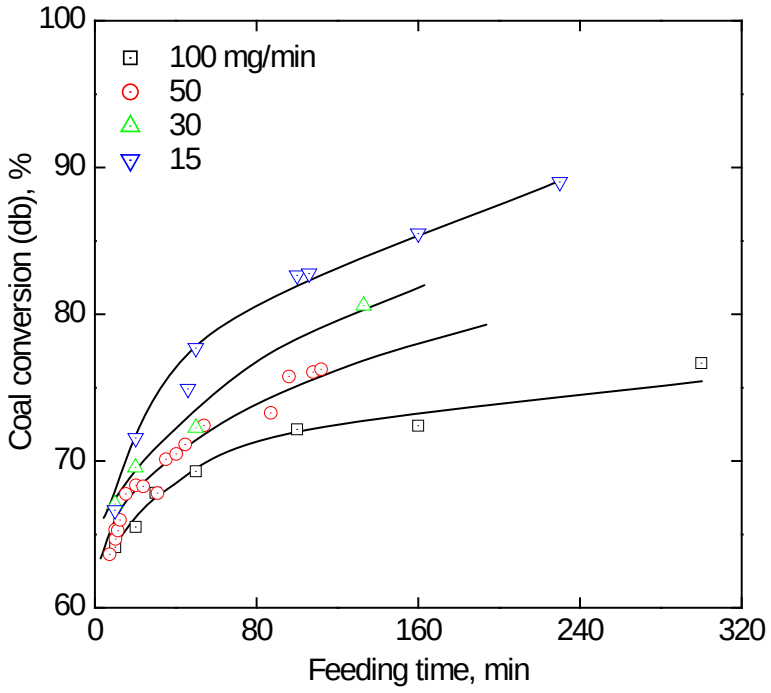

Figure 4-1. Coal conversion as a function of feeding time during the gasification in steam at 800 °C with continuous volatile-char interactions at different feeding rates.

The abundant H radicals could inhibit char conversion by occupying reactive sites, changing char structure and changing retention/concentration of catalytic species (e.g. Na) in char. The changes in char structure shown in the previous chapter were partially responsible for the low char reactivity at the later stage of feeding time. However, the Na (the main inherent catalyst) concentration in char shown in Figure 4-2 did not seem to change with different volatile-char interaction time. This implies that the enhanced release of catalytic species by volatile-char interactions was completed in a very short period after coal particles were fed into the reactor. In the meanwhile, the Mg and Ca concentrations increased with increasing feeding time (volatile-char interaction time). This again indicates that the catalytic effects from Mg and Ca were very limited as the reaction rate significantly decreased at the late stage of feeding time.

The effect of H radical occupying on reactive sites could not be figured out by only looking at the data at a single feeding rate. Its important role could be clearly seen when we compared the char conversion trendlines from different feeding rates. Char structure did not change significantly for the chars prepared at different feeding rates (see Figure 3-1). In addition, the Na concentration was almost the same for the char prepared from different feeding rates while Mg and Ca for 100 mg/min showed lower concentration than others as is shown Figure 4-2. Therefore, the distinctly different char conversion rate must come from the different extents of H radical occupation on those reactive sites. High feeding rates meant high concentrations of volatiles and therefore H radicals. The more reactive sites occupied by H radicals, the less reactive sites will be available to react with steam.

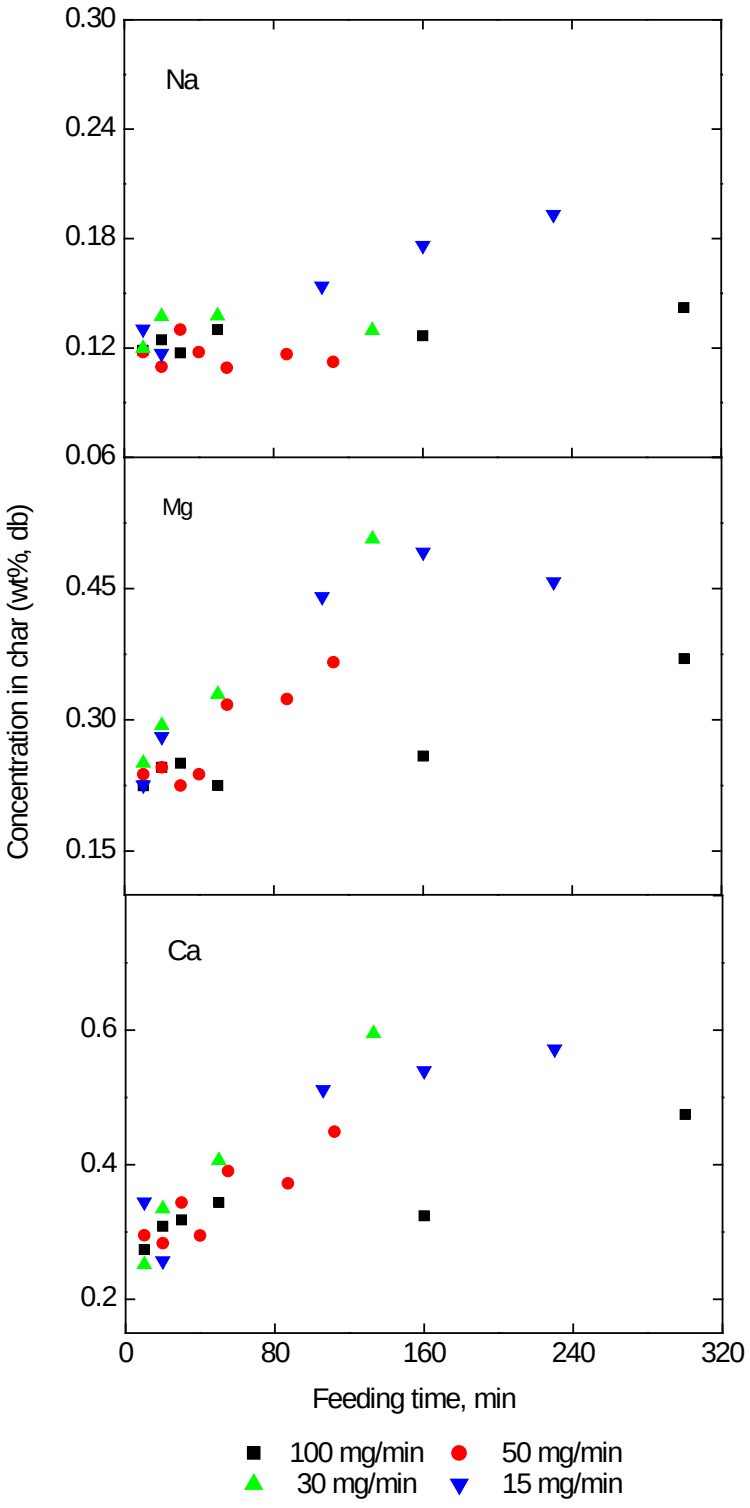

Figure 4-2. AAEM concentration in char as a function of feeding time during the gasification in steam at 800 °C with continuous volatile-char interactions at different feeding rates.

4.2.2 Char conversion during gasification in steam in the absence of volatile-char interactions

Figure 4-1 shows that the char was gasified very slowly in steam at the late stage of feeding time. The discussion above indicates that two reasons should be responsible for this. Firstly the proportion of aged chars increased with increasing feeding time. Secondly H radical occupation on reactive sites slowed down char gasification. Following that, we were keen to know if the reactivity could be improved/recovered in the absence of radicals (volatile-char interactions) in order to understand the relative importance of these two reasons. Therefore, another series of experiments (see Figure 4-3) were carried out. Using a feeding rate of 100 mg/min, two separate points of feeding times were selected as the initial points for further comparison. One point at 50 min in the early stage of feeding was selected while the other one was chosen at 160 min. At the end of each feeding time, the feeding of coal into reactor was suddenly stopped and the char was then gasified in steam in the absence of volatile-char interactions.

Clearly, once the coal feeding (the source of volatiles and radicals) was stopped, the char which was very difficult to be gasified by steam in the presence of volatile-char interactions could be gasified at a very high reaction rate. After about 40 min, the char gasification was somewhat slowed down, but still much faster than that in the presence of volatile-char interactions. It appears that the selection of the initial feeding time had no significant effects on the following gasification rate in steam although the chars from short feeding time (50 min) showed a slightly higher reactivity.

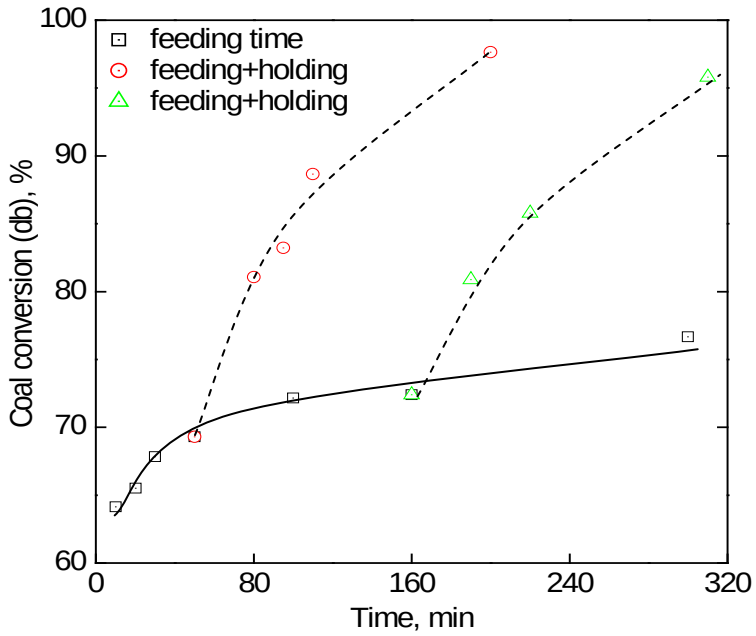

Figure 4-3. Char conversion as a function of time. Solid line: the chars were prepared from continuous volatile-char interactions at 100 mg/min at 800 °C; Dashed line: the chars were prepared from gasification in steam in the absence of volatiles after a period of feeding (50min or 160 min).

The ending of coal feeding resulted in the termination of producing volatiles and corresponding H radicals. When there was a shortage of H radicals on char surface, the reactive sites would be free for reacting with steam at a faster rate. The retrieval of high char reactivity in situ indicates the less importance of char structure at the late stage of feeding in terms of char conversion inhibition, compared to the reactive sites occupation mechanism. However, the slight increase in the proportion of large aromatic ring systems from 50 min feeding to 160 min shown in Figure 3-1 has also led to the slight decrease in char reactivity in the absence of volatile-char interactions. This

demonstrates that the role of char structure in affecting char reactivity could not be ignored.

4.2.3 Char reactivity in air

Chars were collected after the gasification in steam for reactivity measurement in air at 400 °C using TGA. As is shown in Figure 4-4, the specific reactivity fell with increasing volatile-char interaction time for the feeding rates from 100 to 30 mg/min. However, no trend can be seen after 10 min feeding when the feeding rate was further decreased to a very low level of 15 mg/min.

The reduction in the ex-situ char reactivity with increasing feeding time indicates that the changes in char structure and/or char AAEM concentration could have taken place during the gasification in steam. The changes in char structure have been detailed in the previous chapter, which broadly agreed with the reactivity trendlines shown in Figure 4-4. In other words, the reduction in the abundance of small aromatic ring systems has contributed to the decreasing char reactivity as a function of volatile-char interaction time (feeding time). However, the catalytic role of the inherent AAEM (especially Na for Victorian brown coal) should always be examined to understand the changes in char reactivity [19-22]. Therefore, the specific reactivity was plotted as a function of Na concentration shown in Figure 4-5. Immediately, it could be seen that the change in the ex-situ char reactivity did not depend only on the Na concentration for the chars prepared from high feeding rates (30-100 mg/min). For a given Na concentration, the char reactivity decreased

with increasing feeding time (volatile-char interaction time). Therefore, the change in char structure was actually playing a key role in determining the

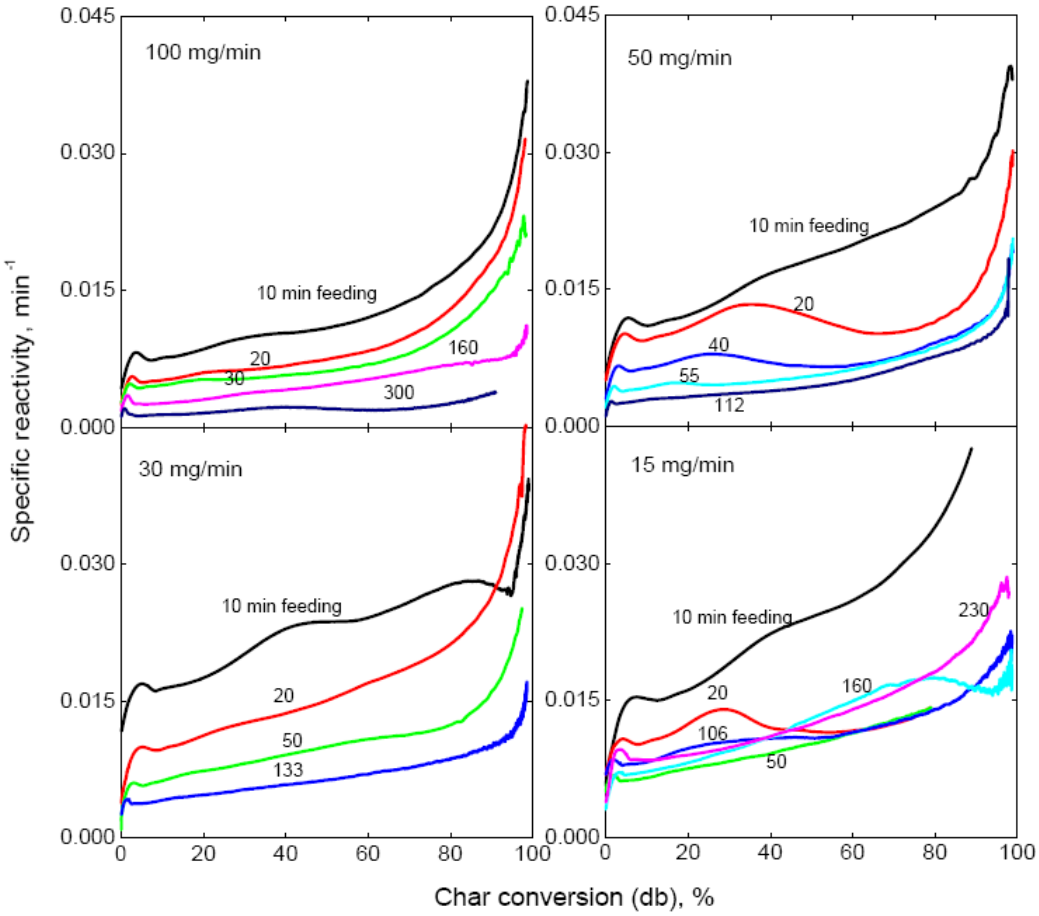

Figure 4-4. Specific reactivity in air at 400 °C as a function of char conversion. Chars were prepared from the gasification in steam with continuous volatile-char interactions at different feeding rates at 800 °C.

ex-situ char reactivity in air for the chars prepared in the presence of volatile-char interactions in steam, but not for the very low feeding rate, e.g. 15 mg/min. For such a low feeding rate, it seems that the char reactivity relied on the Na concentration very much after 10 min feeding. This implies that in this case the change in char structure as a function of feeding time (15 mg/min) in

Figure 3-1 did not result in the significant change in char reactivity. This might be due to the fact that the extent of transformation from the small aromatic ring systems to large ones was not very intensive. Furthermore, the effect of H radicals on AAEM distribution in char could be possibly different when the radical concentration from 15 mg/min feeding rate was compared with that from higher feeding rates.

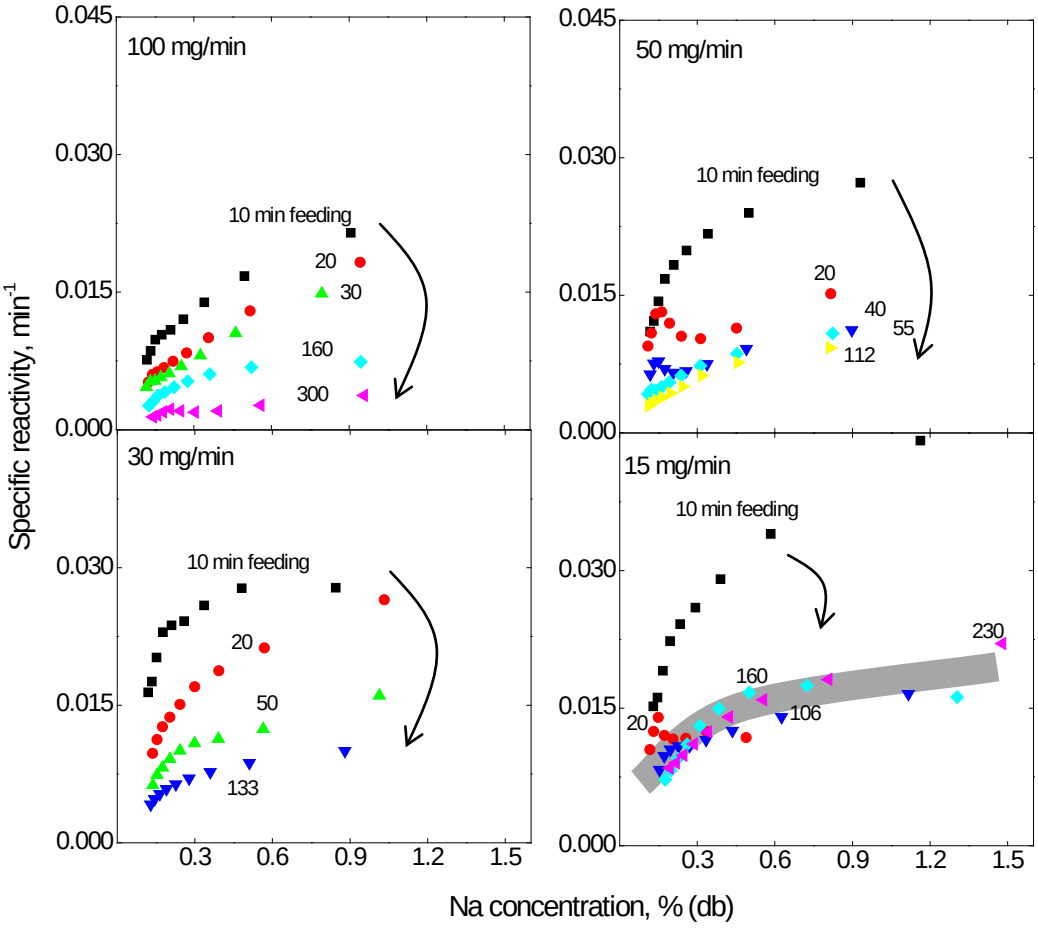

Figure 4-5. Specific reactivity in air at 400 °C as a function of Na concentration. Chars were prepared from gasification in steam with continuous volatile-char interactions at different feeding rates at 800 °C.

Similarly, the *ex-situ* char reactivity in air at 400 °C was measured after the chars were gasified in steam at 800 °C in the absence of volatile-char interactions as is shown in Figure 4-6. It is interesting to note that the char reactivity in air obviously increased as holding time (gasification time) in steam increased based on a feeding time of 50 min. The chars with initial 160 min feeding gave very similar reactivity which still could be discernable to increase with increasing holding time in steam.

The volatilisation of inherent catalysts was very limited in the absence of volatile-char interactions, in agreement with the previous studies [24, 25]. The limited volatilisation caused increasing concentration of Na as char was substantially removed (see initial datum points in Figure 4-6). This appears to be the cause for the rising char reactivity with increasing gasification time in steam, which was supported by the dependence of the reactivity on the concentration of Na shown in Figure 4-7. The data in Figure 4-7 simultaneously indicate that the char structure only played a minor role for the reactivity of char prepared in the absence of volatile-char interactions. However, the char reactivity from Figure 4-6 (A) was generally higher than that from that in Figure 4-6(B). This should be due to the difference in char structure. This is because Figure 3-1 showed that the ratio between small and large aromatic ring systems for the char at 50 min feeding was slightly higher than that for the char at 160 min feeding. The little difference in char structure has resulted in a relatively big difference in char reactivity, which stressed the importance of initial char structure before stopping volatile-char interactions for the subsequent *ex-situ* char reactivity.

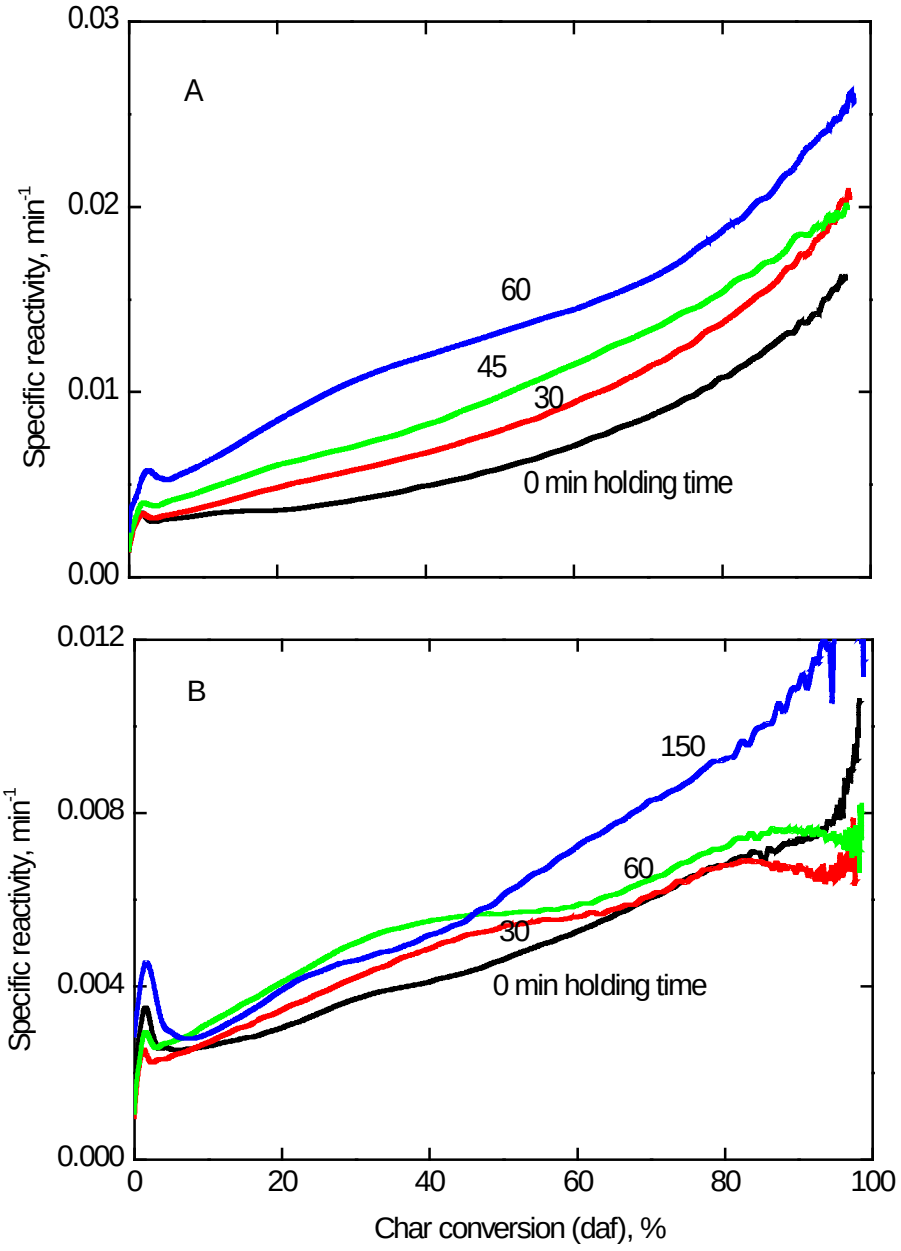

Figure 4-6. Specific reactivity in air at 400 °C as a function of char conversion. Chars were prepared from gasification in steam for different holding time (without volatile-char interactions) after 50 (A) and 160 (B) min feeding respectively at 800 °C.

In addition, the gasification in steam in the absence of volatile-char interactions has given a decreasing reaction rate with increasing gasification time shown in Figure 4-3. The char collected after the longer gasification time showed a higher reactivity in air than that after the shorter gasification time. In other words, the char showing low reactivity in steam gave high reactivity in air. This strongly suggests that the reactive sites in char reacting with steam could be very different from that with oxygen, which was in agreement with our previous study [11, 26].

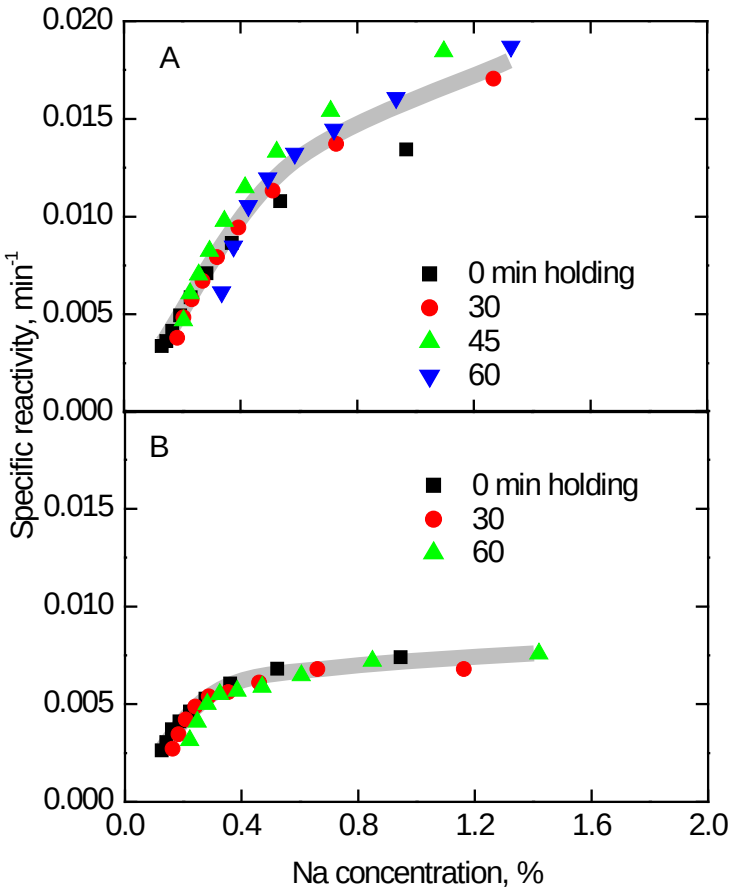

Figure 4-7. Specific reactivity in air at 400 °C as a function of Na concentration. Chars were prepared from gasification in steam for different holding time (without volatile-char interactions) after 50 (A) and 160 (B) min feeding respectively at 800 °C.

4.3 Conclusion

The volatile-char interactions significantly inhibited char conversion during the gasification in steam. The change in char structure greatly affected char conversion at the early stage of feeding time, while the H radical occupying on reactive sites was the main reason for the low char reactivity, especially at the late stage of feeding time.

The subsequent *ex-situ* char reactivity in air was dominated by char structure when the chars were prepared with continuous volatile-char interactions. On the contrary, the catalyst of Na played a crucial role for the reactivity of chars prepared in the absence of volatile-char interactions. In addition, the reaction between char and steam might possibly follow a different mechanism from that between char and oxygen.

4.4 **Reference**

[1] Takarada T, Nabatame T, Ohtsuka Y, Tomita A. Energy Fuels1987;1:308.

[2] Takarada T, Nabatame T, Ohtsuka Y, Tomita A. Ind Eng Chem Res 1989;28:505.

[3] Quyn DM, Wu H, Hayashi J-i, Li C-Z. Fuel 2003;82:587.

[4] Wang J, Takarada T. Energy Fuels 2001;15:356.

[5] Suzuki T, Ohme H, Watanabe Y. Energy Fuels 1992;6:336.

[6] Suzuki T, Ohme H, Watanabe Y. Energy Fuels 1992;6:343.

[7] Chen SG, Yang RT. J Catal 1992;138:12.

[8] Chen SG, Yang RT. J Catal 1993;141:102.

[9] Chen SG, Yang RT. Energy Fuels 1997;11:421.

[10] Wu H, Hayashi J-i, Chiba T, Takarada T, Li C-Z. Fuel 2004;83:23.

[11] Wu H, Li X, Hayashi J-i, Chiba T, Li C-Z. Fuel 2005;84:1221.

[12] Li C-Z. Fuel 2007;86:1664–1683.

[13] Wu H, Li X, Hayashi J-i, Chiba T, Li C-Z. Fuel 2005;84:1221.

[14] Ohtsuka Y, Asami K. Energy Fuels 1995;9:1038.

[15] Li X, Hayashi J-i, Li C-Z. Fuel 2006;85:1700.

[16] Li X, Li C-Z. Ranliao Huaxue Xuebao 2005;33:385.

[17] Li X, Hayashi J-i, Li C-Z. Fuel 2006;85:1509.

[18] Li X, Li C-Z. Fuel 2006;85:1518.

[19] Wu H, Quyn DM, Li C-Z. Fuel 2002;81:1033–9.

[20] Quyn DM, Wu H, Li C-Z. Fuel 2002;81:143–9.

[21] Quyn DM, Wu H, Bhattacharya SP, Li C-Z. Fuel 2002;81:151–8.

[22] Li X, Wu H, Hayashi J-i, Li C-Z. Fuel 2004;83:1273–9.

[23] Bayarsaikhan B, Sonoyama N, Hosokai S, Shimada T, Hayashi J-i, Li C-Z, Chiba T. Fuel 2006;85:340-349.

[24] Sathe C, Pang Y, Li C-Z. Energy Fuels 1999;13:748.

[25] Li C-Z, Sathe C, Kershaw JR, Pang Y. Fuel 2000;79:427.

[26] Bayarsaikhan B, Hayashi J-i, Shimada T, Sathe C, Li C-Z, Tsutsumi A, Chiba T. Fuel 2005;84:1612.

CHAPTER 5

Effects of intra- and inter-particle volatile-char interactions on char evolution during gasification in steam using mallee woody biomass

Summary

Volatile-char interactions have shown significant effects on char evolution during the gasification of brown coal in steam. Biomass features even higher volatile and aliphatic contents as well as more reactive char, and thus the volatile-char interactions during biomass gasification could be also very dramatic. Moreover, large particles are often used in biomass utilisation processes. Intra-particle volatile-char interactions in a large particle may become an important issue during the diffusion of nascent volatiles out of the particle.

This study is to examine the effects of volatile-char interactions on changes in char properties during biomass gasification in steam by varying biomass particle size and heating rate. Two novel fluidised-bed/fixed-bed quartz reactors were used for conducting the slow and fast heating experiments. The chars produced from the experiments were then characterised for their structural features, AAEM retention and char reactivity. It was found that the inter- and intra-particle volatile-char interactions have affected the char conversion considerably under both slow and fast heating conditions. The changes in char properties due to the changes in biomass particle size were only significant during the gasification at fast heating rates. Part of data in this chapter was obtained by Dr. Mohammad Asadullah in a collaborative study.

5.1 Introduction

Biomass gasification is one of the technologies to meet growing demand for electricity, hydrogen, chemicals and liquid fuels [1]. The process has a number of advantages in respect of sustainable development. However, the biomass gasification in steam faces a number of technical challenges to become a commercial renewable energy technology. In the steam gasification system, when biomass is exposed to high temperatures (> 700 ^{o}C), a complex mixture of steam, vapours of a large number of organic compounds and gaseous products evolves, leaving behind a solid mass (char). The organic vapours and char then take part in the gasification/reforming reactions with the gasifying agents. Enhancing the solid char gasification rate one of the most important challenges. The interactions of volatiles (the organic vapours) with char have shown a great inhibition to char conversion during the gasification of brown coal [2]. For biomass, intra-particle volatile-char interactions in the devolatilisation step can be significant when large biomass particles are used. The intra-particle volatile-char interactions might be even more intensive than the inter-particle volatile-char interactions as the volatiles and char inside particles are more “fresh” and reactive. Additionally, the volatile concentration is higher inside particle compared to that outside, which also enhances the interactions between volatiles and char.

During the process of intra-particle volatile-char interactions, the organic and AAEM vapours can re-adsorb on the surface of the porous char. The recombination of AAEM with the char could affect the char reactivity enormously as they are perfect inherent catalysts for gasification [3-4]. Like

inter-particle volatile-char interactions, abundant H radicals can be generated from the thermal cracking/reforming of volatiles during the intra-particle volatile-char interactions. The H radicals could likely induce char structural changes drastically as shown in Chapter 3. The changes in char structure will in turn affect AAEM retention/dispersion and chemical/physical forms in char [5]. Therefore, it is essential to gain insights into the details of the structural features of char prepared during the steam gasification of biomass under the conditions featuring inter- and intra-particle volatile-char interactions.

However, understanding the changes in char structure had been made difficult by the lack of suitable analytical techniques to quantify the carbon-skeleton structural features of coal/biomass char [6]. The structural features of chars have been investigated using X-ray diffraction (XRD), FTIR spectroscopy, high-resolution transmission electron microscopy (HRTEM) and Raman spectroscopy [7-11]. The XRD technique is suitable to characterize graphite-like carbon materials that have a highly ordered crystalline structure. However, it is evident that the biomass chars are highly disordered carbonaceous materials [12]. The FT-IR spectroscopy precisely identifies the oxygen-containing functional groups in carbon material; however, it is of limited use in exploring the less-polar aromatic structures. Raman spectroscopy is widely used for the characterization of both crystalline and amorphous carbon, because it is sensitive to both of them [7-11]. But the method using Raman technique in the literature was mainly for characterising graphite-like carbon materials. Therefore, a novel Raman spectroscopic method has been developed in our group to characterize the amorphous

carbon [13-20] that will be used in this study to provide information about char structures.

In order to explore the changes in AAEM retention, char structure and reactivity under different extents of inter- and intra-particle volatile-char interactions, different types of chars prepared from different particle sizes at different heating rates were analysed respectively. The results indicate that the particle size of biomass plays an important role in the evolution of char properties (i.e. char structure, AAEM retention and char reactivity) during the gasification in steam at fast heating rates.

5.2 Results and discussion

5.2.1 Char conversion profiles

Experiments for the slow heating rate (10 ^{o}C/min) and fast heating rates were conducted in two different types of fluidised-bed quartz reactors, which were detailed in Chapter 2. In the case of the slow heating rate, ~5 g wood biomass particles were pre-loaded into the reactor before heating up at 10 ^{o}C/min to the desired temperatures. In the case of fast heating rates, the biomass particles were fed into reactor after the desired temperature inside reactor had been achieved.

Figure 5-1 shows biomass conversion as a function of particle size during the gasification in steam at both slow and fast heating rates. Biomass conversion under fast heating rates was more significant than that under a slow heating rate for all the particle sizes. Increasing particle size has led to decreased lower biomass consumption for a given heating rate and temperature. As expected, biomass conversion at 700 ^{o}C was cleary lower than that at 800 ^{o}C.

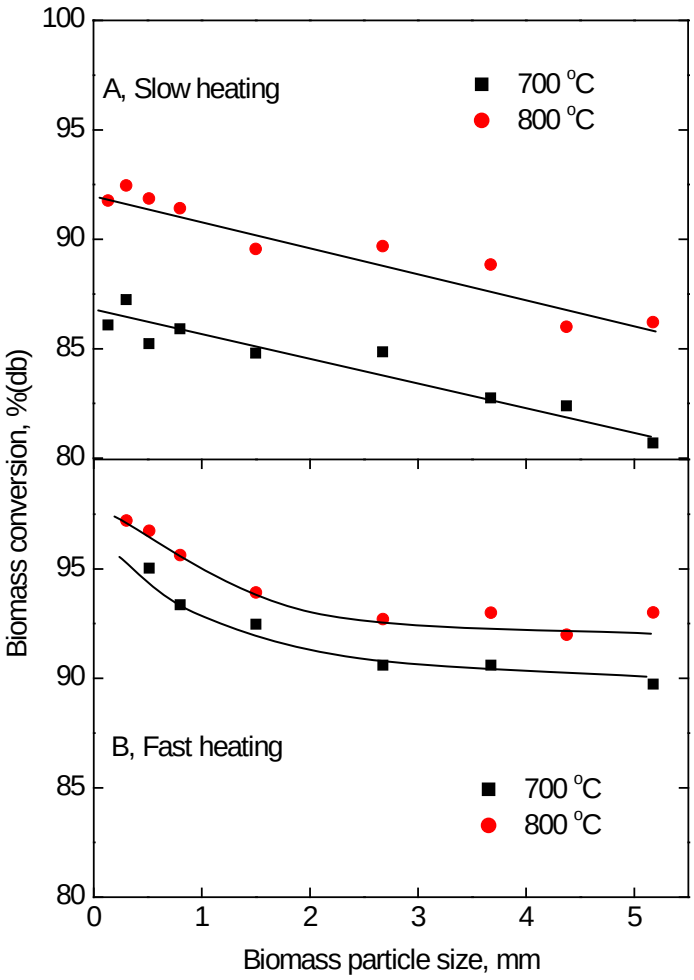

Figure 5-1. Biomass conversion as a function of biomass particle size during the gasification in steam at the different heating rates and temperatures.

The change in biomass conversion due to heating rate could be attributed to two reasons. Firstly the extent of biomass devolatilisation at the fast heating rates would be high. When the biomass particles are suddenly fed into a very hot fluidised sand bed (700 or 800 ^{o}C in this case), many chemical bonds including cross-links break down in a short period and form numerous fragments. These fragments can be released as volatiles. In contrast, the bonds were slowly cracked down under the slow heating conditions. The fragment would not be volatilised unless all the bonds between one fragment

and char matrix are cracked down at the same time. Secondly the “self-gasification” [14, 21] of the chars by the volatiles was likely to be a cause of this increase in char conversion at the fast heating rates. At fast heating rates, the volatiles were released at the reaction temperature, and the moisture in the raw sample as well as steam and CO_2 from the primary pyrolysis of the biomass could partially gasify the char surrounded by the volatiles. Some steam and CO_2 might also be formed from the thermal cracking of light hydrocarbons and tar at temperatures higher than 700 ^{o}C. However, at a heating rate of 10 K min^{-1}, these volatiles would have slowly sweped out of the reactor before the solid reached high enough temperatures (e.g. 650 ^{o}C) for the gasification reactions to take place.

The variation in biomass conversion with biomass particle sizes was indeed a result of the difference in heating rate and the diffusion resistance for volatiles. There must have been a gradual temperature distribution from the external surface to the centre of the particle. The heat transfer from the external surface to the centre part could not be immidiate as the thermal conductivity of biomass/char was low. Therefore, the average heating rate for small biomass particles was higher than that for large biomass particles. Clearly, the transportation time (intra-particle volatile-char interaction time) for large particles was certainly longer than that in small ones. This gave the volatiles more chances to recombine with char, thus reducing biomass conversion.

5.2.2 Change in char structure

The total observed Raman peak areas between 800 and 1800 cm^{-1} of chars prepared at slow and fast heating rates are shown in Figure 5-2 as a function of biomass particle size. Particle size within the range examined was not an apparent factor affecting the total Raman intensity. At the fast heating rates, high temperature dramatically decreased the total intensity. The total intensity was almost the same from 700 to 800 ^{o}C at slow heating rate. The effect of heating rate on the total intensity was complex, but depending on temperature.

The total observed Raman peak area is determined by Raman scattering ability and light absorptivity of the char [15-19]. At fast heating rates, the total observed peak area decreased substantially from 700 to 800 ^{o}C, which was at least partially due to the increase in the proportion of large aromatic ring systems. Moreover, the char matrix from fast heating rates (especially at 800 ^{o}C) was very vulnerable as it was relatively “fresh” (newly-formed from the decomposition of biomass). The oxygen complex from volatiles on char surface could easily decompose Therefore, the O-containing groups in the char could be less significant, resulting in the low observed total Raman intensity for the char prepared from the fast heating rates at 800 ^{o}C.

However, at the slow heating rate, there was no apparent change in the observed total intensity with increasing temperature from 700 to 800 ^{o}C. For slow heating rate, the gasification reaction between char and steam at 800 ^{o}C could enrich the O-containing functional groups in char structure. The O-containing groups could enhance the observed total Raman intensity via

exerting resonance effects on aromatic ring systems [20], hence balancing the adverse effects of the increased acromaticity on the observed Raman intensity.

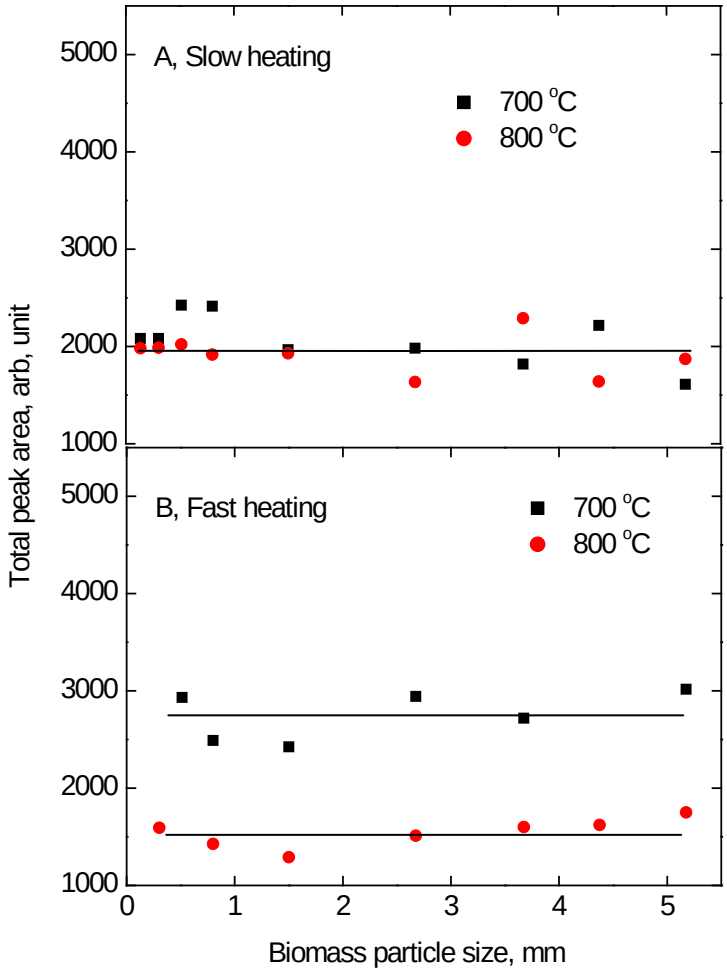

Figure 5-2. Total observed Raman peak area/intensity between 800 and 1800 cm^{-1} as a function of biomass particle size during gasification at different heating rates and temperatures.

The curve-fitting (deconvolution) of char Raman spectra revealed that G_R, V_L, V_R and D are four most important bands. G_R represents small aromatic ring systems (3-5 fused rings) while D reflects large aromatic ring systems (no less than 6 fused rings) [15, 16]. $G_R+V_L+V_R$ together symbolize the amorphous carbon structure, including aliphatics and carboxylates. Therefore, the changes in band area ratios, I_{GR}/I_D and $I_{(GR+VL+VR)}/I_D$, could be used as an expression for the changes in the relative abundance of small and large aromatic ring systems in char.

Figures 5-3 and 5-4 show that I_{GR}/I_D and $I_{(GR+VL+VR)}/I_D$ changed as a function of biomass particle size during gasification in steam at different heating rates and temperatures. The ratios increased with increasing heating rate and decreasing temperature. The increase in particle size caused increase and then decrease in the ratios of I_{GR}/I_D and $I_{(GR+VL+VR)}/I_D$ for the condition of 800 ^oC and fast heating rate.

Increasing temperature from 700 to 800 ^oC during gasification in steam may decrease the ratio I_{GR}/I_D and $I_{(GR+VL+VR)}/I_D$ by two ways. Firstly, the preferential consumption by steam of small aromatic ring systems could result in the reduction in the relative abundance of small aromatics. Secondly, the small aromatic ring systems could be converted into large ones via condensation reaction when the temperature increased. By comparing Figure 5-1 to 5-3 and 5-4, it is not hard to find that the ~5% more char conversion from 700 to 800 ^oC was not accountable for the significant decrease in the ratios even if we assumed that the 5% consumption was all small aromatics.

Therefore, the transformation from small aromatic ring systems to big ones must have taken place when the temperature increased.

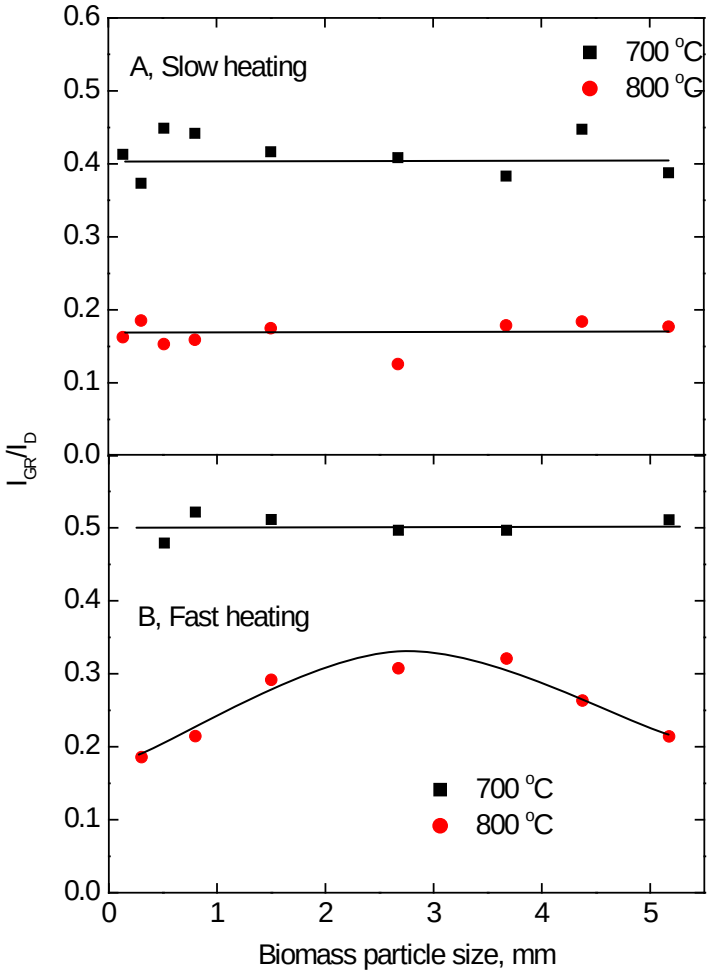

Figure 5-3. Raman peak area ratio I_{GR}/I_D as a function of biomass particle size during gasification at different heating rates and temperatures.

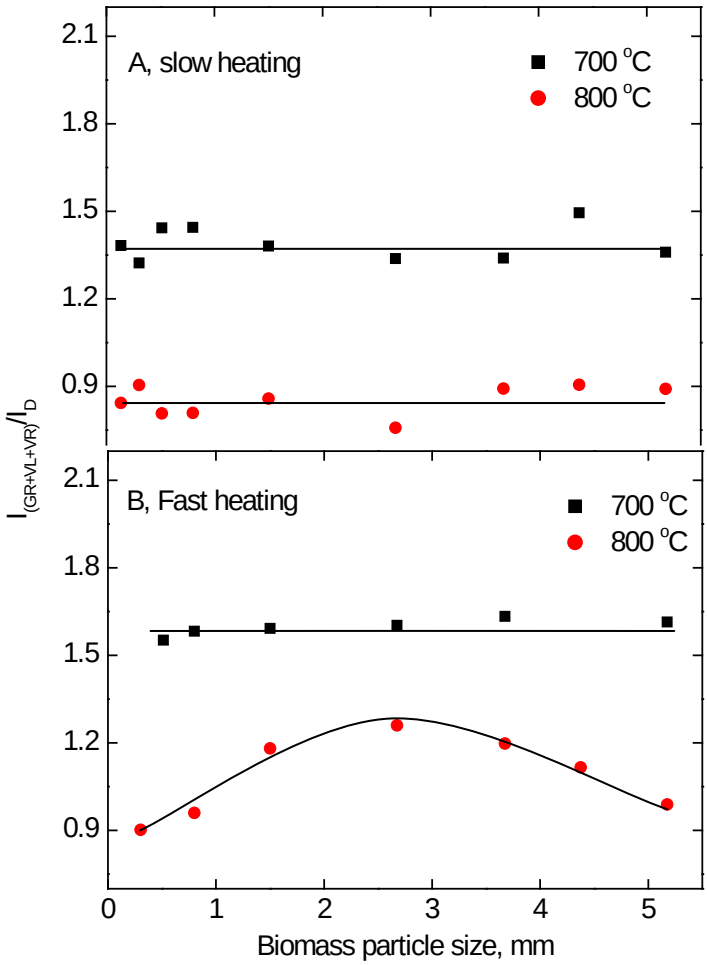

Figure 5-4. Raman peak area ratio $I_{(GR+VL+VR)}/I_D$ as a function of biomass particle size during gasification at different heating rates and temperatures.

The low I_{GR}/I_D and $I_{(GR+VL+VR)}/I_D$ ratios at the slow heating rate could be due to the more significant secondary reactions and associated char structural changes during the slow gasification process. Compared to the slow heating rate, the char derived from the fast heating rates was quenched in a short time after being fed into the reactor. Consequently, the condensation reaction time for the char from fast heating rates was shorter than that for the char from the

slow heating rate. Additionally, the H radicals from the thermal cracking/reforming of volatiles during the gasification at fast heating rates might, to a certain extent, inhibit the preferential consumption of the small aromatic ring systems by occupying on the reactive sites.

In terms of the effects of biomass particle size, the trend from 800 ^{o}C under fast heating rate need to be specially discussed. The ratios I_{GR}/I_D and $I_{(GR+VL+VR)}/I_D$ went to a maximum value at about 2.5 mm of particle size. It is likely that the large aromatic ring systems could be "opened" by steam at 800 ^{o}C (this will be particularly investigated in next chapter). The "opening" process was largely affected by H radical (from the thermal cracking/reforming of volatiles) concentrations inside particle. The H radicals could activate the aromatic ring systems, thus creating more small aromatics. With increasing biomass particle size, the H radicals inside particles could be more abundant due to enhanced volatile-char interactions. More H radicals would create more small aromatic ring systems with steam. Therefore, the ratios I_{GR}/I_D and $I_{(GR+VL+VR)}/I_D$ increased. With increasing biomass particle size further, the extent of intra-particle volatile-char interactions was substantially significant, which was similar to the effect of increasing the thickness of char bed in chapter 3. The very high concentration of H radicals could then be enough to facilitate the growth of aromatic ring systems. Thus the ratios I_{GR}/I_D and $I_{(GR+VL+VR)}/I_D$ decreased from the particle size of 2.5 mm. It is also understandable that the trend could be only seen during the gasification in steam at 800 ^{o}C because the presence of steam at the relatively high temperature could reform volatiles and facilitate the generation of H radicals.

5.2.3 AAEM retention

Figure 5-5 shows the changes in AAEM retention as a function of biomass particle size during gasification in steam at the slow heating rate. The AAEM retention was calculated based on their contents in dry biomass. The effect of temperature (from 700 to 800 ^{o}C) on AAEM retention was not significant, but discernable. There was no/little change in AAEM retention with increasing the biomass particle size.

For gasification in steam at 700 and 800 ^{o}C at the slow heating rate, the AAEM retention was generally as high as 60-90 wt%. The thermal cracking or gasification at a slow heating rate of 10 ^{o}C/min was a very slow process; this would be in favour of AAEM recombination as well as formation of inorganic salts (e.g. carbonates). Additionally, the cell structure of biomass may act as a 'cage' for the AAEM species to prevent their volatilisations [21, 22].

The negligible effect of particle size on AAEM retentions during the gasification at the slow heating rate indicates that the secondary reaction between AAEM (in volatiles) and char affected AAEM retentions very little. The secondary reaction certainly took place to some extent, especially inside large biomass particles, but it did not cause a high retention for most AAEM species. As we mentioned above, the inter-particle volatile-char interactions for small biomass particles were more significant due to char bed formation than large ones. Thus the small biomass particles did not show a lower retention for most AAEM species than did the large biomass particles which featured higher extent of intra-particle volatile-char interactions. However, the effect of intra- and inter-particle AAEM-char interactions on AAEM retentions

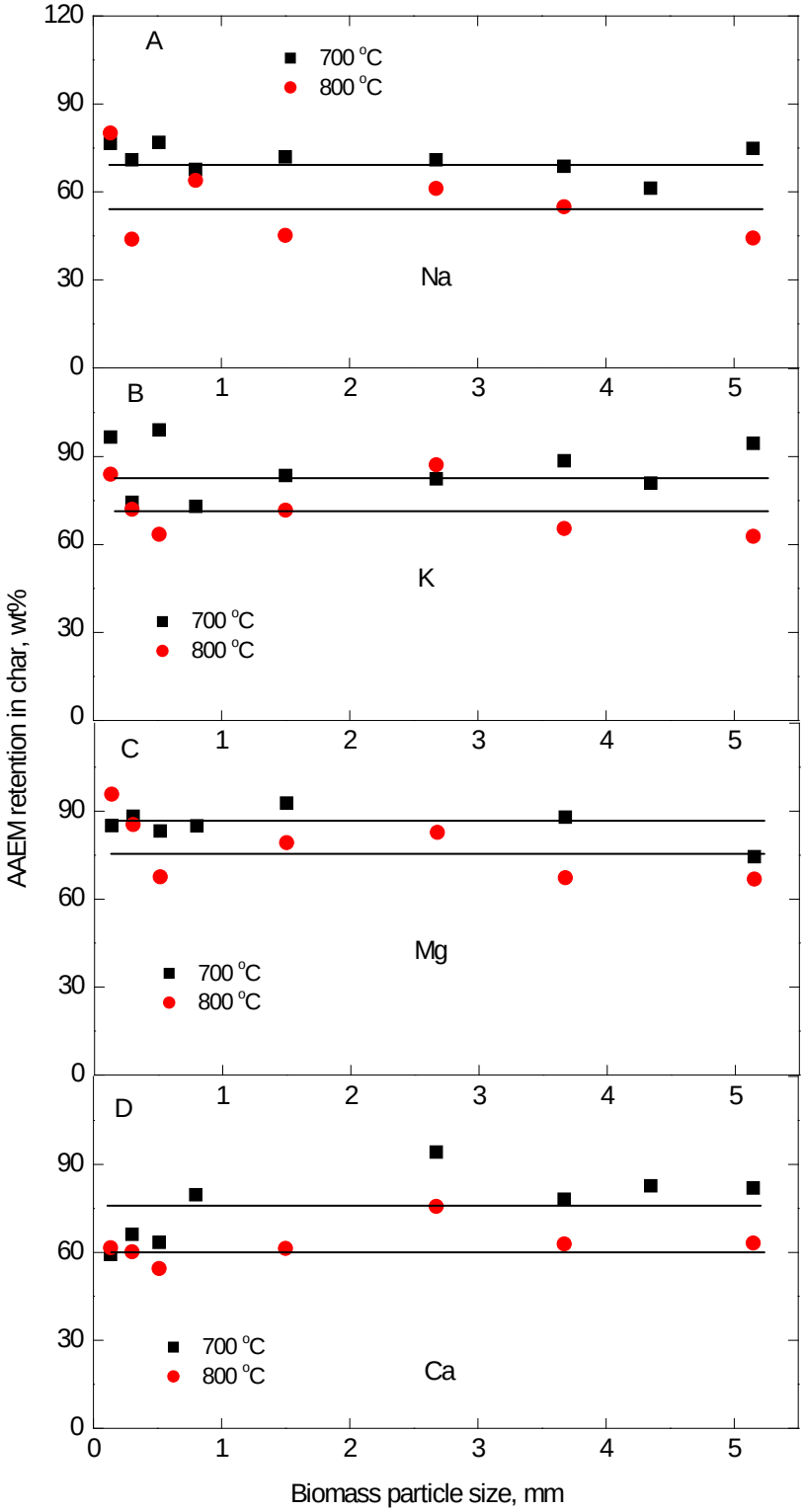

Figure 5-5. AAEM retention as a function of biomass particle size during gasification under the slow heating rate of 10 °C/min.

was not very intensive because only small amount (10-30 wt%) of AAEM was gradually released from char/biomass matrix during the gasification at the slow heating rate. The concentration of AAEM in volatiles was thus very low at any moment, compared to that in the case of fast heating rates. At a slow heating rate, there are little inter-particle volatile-char interactions. Even the intra-particle volatile-char interactions would be limited because volatiles are released at a much lower temperature than the temperature at which volatile-char interactions would have any effect.

Figure 5-6 shows AAEM retention at fast heating rates. Compared to the data at the slow heating rate, two notable features in the data of Figures 5-6 have been observed: the AAEM retention in char increased with increasing biomass particle size for both 700 and 800 ^{o}C experiments and it decreased with increasing gasification temperature in most cases.

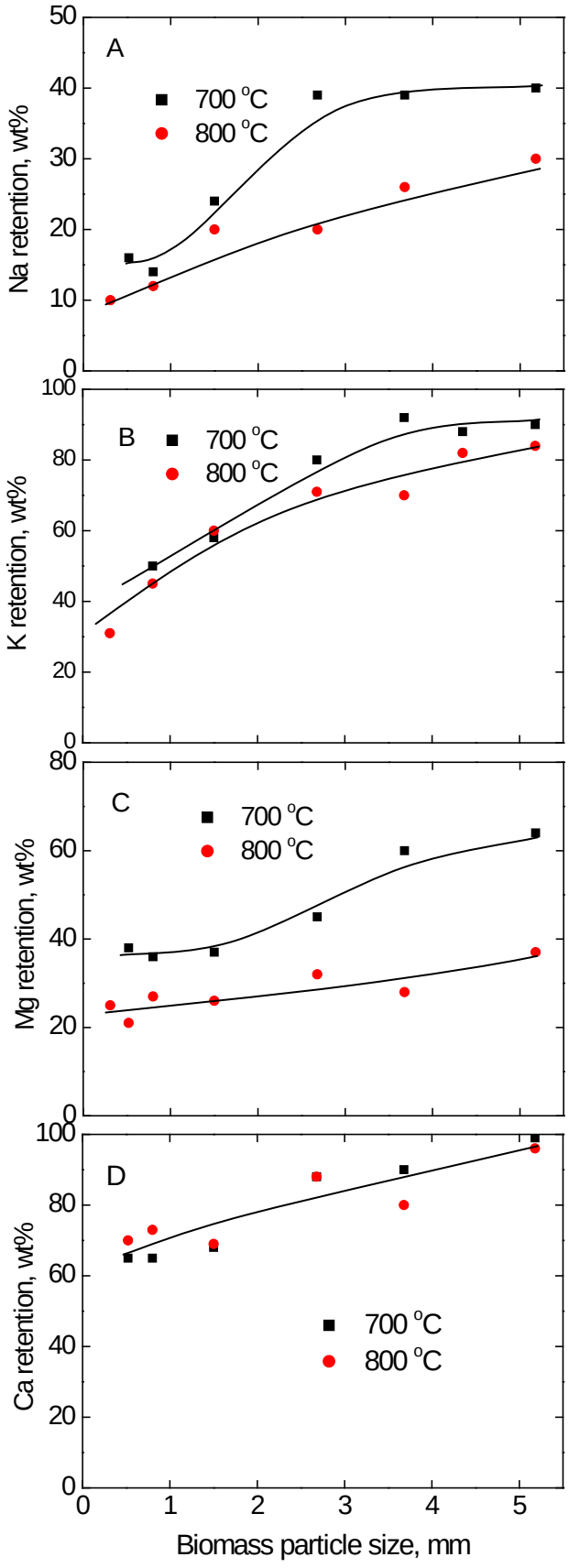

Figure 5-6. AAEM retention as a function of biomass particle size during gasification under the fast heating rates.

The variation in the retention of AAEM species in char derived from variable particle size of biomass during the gasification at fast heating rates could be understood by the following considerations. In biomass, AAEM (Na, K, Mg and Ca) mainly exist as inorganic forms. During devolatilization at the fast heating rates, the metal species in the vapour phase considerably recombines through the secondary reactions with chars. These processes were indeed intra-particle and inter-particle volatile-char interactions. The intra-particle and inter-particle volatile-char interactions at fast heating rates were much stronger than that under the slow heating rate because huge amounts of volatiles were generated in a very short time in the case of fast heating condition. This was also one of the main reasons for the observed difference in the trend of AAEM retention between slow and fast heating rates.

At fast heating rates, for the smaller particle of biomass, the pressure of vapour phase inside the char was very low due to the low mass transfer resistance, and thus the possibility of secondary recombination of AAEM species inside the particles was small. Comparatively, the much more significant recombination in the large biomass particles than that int the small ones during the fast heating rates could be expected. Furthermore, the true heating rate in the large particles was slower than that in the small biomass particles, which would certainly limit the volatilization of AAEM in the large biomass/char particles. Therefore, the AAEM retention increased with increasing biomass particles as shown in Figure 5-6. Clearly, the thermal cracking/reforming reactions at the temperature of 800 ^{o}C could break more bonds between AAEM and Char matrix.

5.2.4 Change in reactivity

Figure 5-7 shows the change in specific reactivity as a function of biomass particle size and temperature for the chars derived from gasification in steam at a slow heating rate. The different sizes of char particles were grounded into similarly fine ones prior to reactivity measurements in air at 370 °C using TGA. Therefore, the resistance of oxygen diffusion for all the samples was supposed to be almost the same and negligibly small.

The most important feature in Figure 5-7 was that the specific reactivity decreased with increasing biomass particle size. Generally, char reactivity was mainly affected by two factors. One is the char structure while the other one is AAEM (catalysts) concentration/dispersion in the char. The change in char structure in Figure 5-4 was not accountable for the change in char reactivity shown in Figure 5-7. This indicates that the inherent catalysts (AAEM) were responsible for the decreasing char reactivity with increasing biomass particle size. Figure 5-5 shows that most of AAEM retention during gasification in steam at the slow heating rate did not really alter with increasing biomass particle size. However, Figure 5-1 shows that the char conversion reduced with increasing biomass particle size. Consequently, AAEM concentration in char decreased with increasing biomass particle size, which at least partially contributed to the decreasing specific reactivity of char at both temperatures of 700 and 800 ^{o}C as is shown in Figure 5-7.

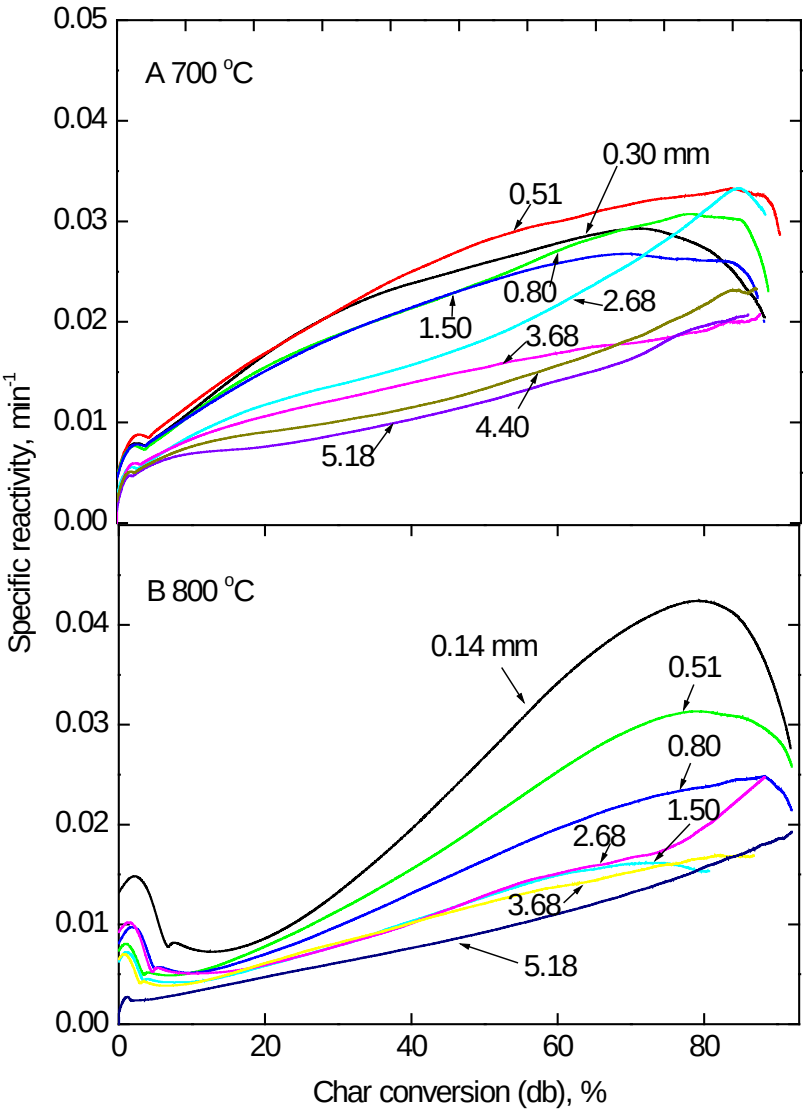

Figure 5-7. Char reactivity as a function of char conversion measured at 370 °C. The chars prepared from different biomass particle sizes at different temperatures in steam gasification under the slow heating of 10 °C/min.

In contrast, the change in char reactivity at the fast heating rates shown in Figure 5-8 was more complex. Firstly, the specific reactivity for the chars prepared from 800 ^{o}C was much lower than that from 700 ^{o}C. This could be due to the difference in char structure shown in Figure 5-4. The proportion of small aromatic ring systems for the chars from 700 ^{o}C was much more abundant than that for the chars from 800 ^{o}C. Small aromatic ring systems (3-5 fused rings) have shown a higher reactivity than large aromatic ring systems (no less than 6 fused rings) [14, 17, 21]. Secondly, the change in char reactivity did not follow a trend with increasing biomass particle size at both temperatures of 700 and 800 ^{o}C. At 700 ^{o}C, the specific reactivity in char increased firstly with increasing biomass particle size, and then decreased with further increasing biomass particle size. The increasing char reactivity with increasing biomass particle size from 0.52 to 1.50 mm was mostly due to the increasing AAEM retention in Figure 5-6 as char structure change could not be observed. However, the continual increasing AAEM retention in Figure 5-6 did not result in continual increase in char reactivity beyond the biomass particle size of 1.5 mm. Instead, the specific reactivity for the char from very large particles decreased. Probably, in the large particle, the re-combination of AAEM inside particles was on the char surface. As mentioned before, the large char particles were all ground into very fine particles prior to the reactivity measurement. When we ground the large particles into very small ones, new surface area was created. Therefore, the AAEM distribution onto the surface of the fine particles after grinding might not be good, thus the efficiency of catalytic effect in this case was negatively affected, resulting in the decreased char reactivity with further increasing biomass particle size.

The reactivity for the chars from 800 ^{o}C generally changed very little with varying biomass particle size although the values did not follow a trend. Each curve fluctuated significantly with increasing char conversion, which indicated the importance of char structure.

The fluctuated reactivity of the same char at different conversion levels reveals that the different domains with distinct structural features in char were formed, in which catalyst species were distributed heterogeneously. The condensed structure was less reactive than amorphous structure. In addition, the existence of catalytic species in condensed carbon species was less preferable and thus they might be enriched in amorphous domain, leading to higher combustion reactivity at the early stage of char conversion in TGA. Furthermore, when amorphous carbon was exhausted in the combustion reaction, the catalytic species moved to the surface of the condensed char structure. The condensed char with the immigrated catalysts showed the high reactivity at the late stage of char conversion.

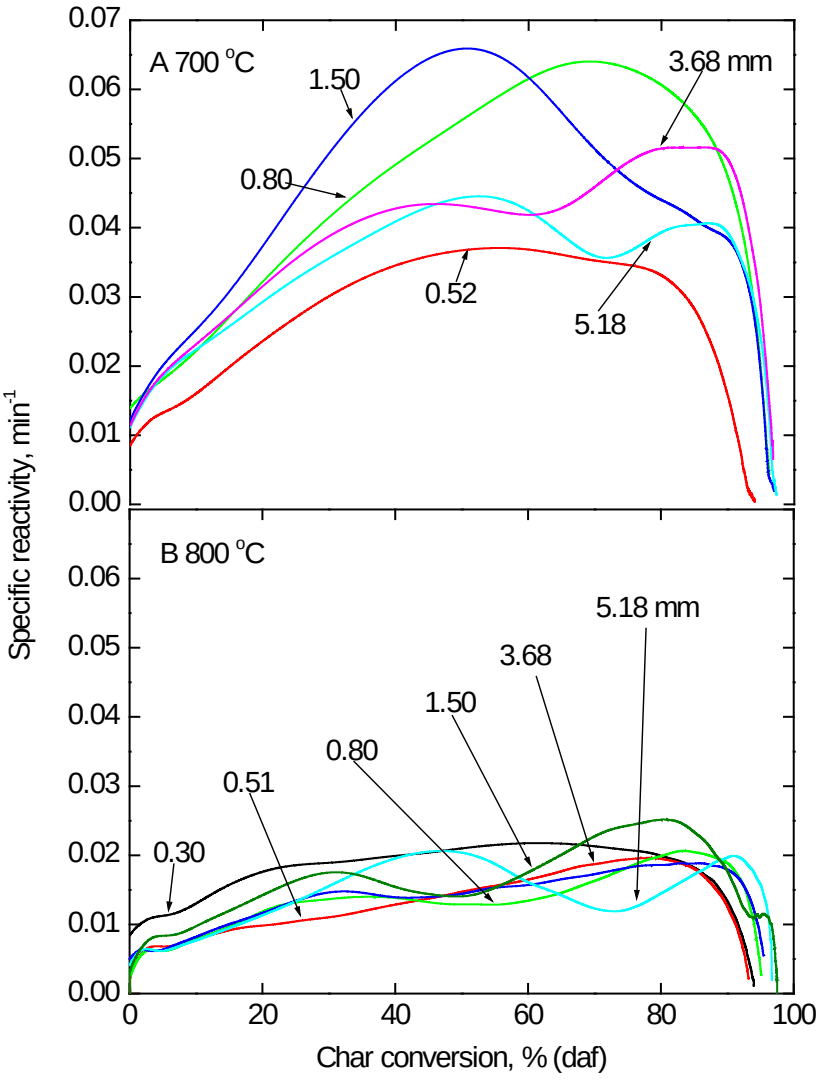

Figure 5-8. Char reactivity as a function of char conversion measured at 370 °C. The chars prepared from different biomass particle sizes at different temperatures in steam gasification under fast heating.

5.3 Conclusions

The secondary reactions due to the volatile-char interactions have caused a low char conversion for large biomass particles in both slow and fast heating rates. The intra-particle volatile-char interactions greatly reduced volatilisation of AAEM in large biomass particles at fast heating rates, but little change in char structure was seen with increasing biomass particle size. The char reactivity for the chars depended on the catalytic species, being largely affected by the nature of heterogeneous structure in char, especially for the chars prepared at fast heating rates.

5.4 References

[1] Li C-Z. Special issue—Gasification: a route to clean energy. Process. Saf. Environ. Prot. 2006; 84: 407–408.

[2] Bayarsaikhan B, Sonoyama N, Hosokai S, Shimada T, Hayashi J-i, Li C-Z, et al. Fuel 2006;85:340-349.

[3] Mermoud F, Salvador S, Van de Steene L, Golfier F. Influence of the pyrolysis heating rate on the steam gasification rate of large wood char particles. Fuel 2006; 85:1473–1482.

[4] Zolin A, Jensen A., Jensen P A, Frandsen F, Dam-Johansen K. The influence of inorganic materials on the thermal deactivation of fuel chars. Energ. Fuel 2001; 15: 1110–1122.

[5] Quyn D M, Wu H, Hayashi J-I, Li C-Z. Volatilisation and catalytic effects of alkali and alkaline earth metallic species during the pyrolysis and gasification of Victorian brown coal. Part IV. Catalytic effects of NaCl and ion-exchangeable Na in coal on char reactivity. Fuel 2003; 82:587–593.

[6] Li C-Z. Some recent advances in the understanding of the pyrolysis and gasification behaviour of Victorian brown coal. Fuel 2007; 86: 1664–1683.

[7] Green P D, Johnson C A, Thomas K M. Applications of laser Raman microprobe spectroscopy to the characterization of coals and cokes. Fuel 1983; 62: 1013-1023.

[8] Cuesta A, Dhamelincourt P, Laureyns J, Martinez-Alonso A, Tascon J. M. D. Raman microprobe studies on carbon materials. Carbon 1994; 32 (8) 1523-1532.

[9] Tuinstra F, Koenig J L. Raman spectrum of graphite. J. Chem. Phys. 1970; 53: 1126-1130.

[10] van Doorn J, Vuurman M A, Tromp P J J, Stufkens D J, Moulijn J A. Correlation between Raman spectroscopic data and the temperature-programmed oxidation reactivity of coals and carbons. Fuel Process Technol. 1990; 24: 407-413.

[11] Zerda T W, Xu W, Zerda A, Zhao Y, Von Dreele R. B. High pressure Raman and neutron scattering study on structure of carbon black particles. Carbon 2000; 38 (3) 355–361.

[12] Sharma R K, Wooten J B, Baliga V L, Hajaligol M. R. Characterization of chars from biomass-derived materials: pectin chars. Fuel 2001; 80:1825-1836.

[13] Li X, Hayashi J-I, Li C-Z. FT-Raman spectroscopic study of the evolution of char structure during the pyrolysis of a Victorian brown coal. Fuel 2006; 85: 1700-1707.

[14] Keown D M, Li X, Hayashi J-I, Li C-Z. Characterization of the structural features of char from the pyrolysis of cane trash using Fourier Transform−Raman spectroscopy. Energ. Fuel 2007; 21: 1816-1821.

[15] Li X, Hayashi J-I, Li C-Z. Fuel 2006;85:1509–1517.

[16] Li X, Li C-Z. Fuel 2006;85:1518–1525.

[17] Li X, Hayashi J-I, Li C-Z. Fuel 2006;85: 1700–1707.

[18] Li X, Li C.-Z. Ranliao Huaxue Xuebao 2005;33:385-390.

[19] McCreery RL. Raman spectroscopy for chemical analysis. New York:Wiley–Interscience; 2000.

[20] Leites LA, Bukalov, SS. J. Raman Spectrosc. 2001; 32:413-424.

[21] Keown D.M, Favas G, Hayashi J.-I, Li C.-Z. Bioresource Technol 2005; 96: 1570.

[22] Keown D. M, Hayashi J.-I, Li, C.-Z. Fuel 2008;87:1187.

[23] Keown D. M, Hayashi J.-I, Li, C.-Z. Fuel 2008;87:1127-1132.

Chapter 6

Change in char structure due to a sudden contact with steam following the pyrolysis of mallee woody biomass

Summary

The discussion in section §5.2.2 indicates that the “unusual” change in char structure occurred during the gasification in steam when large biomass particles were used. Moreover, a paper from our group reported the dramatic change in char structure due to the sudden introduction of steam following pyrolysis using a small size of cane trash biomass.

Therefore, in order to better understand the changes in char structure for different mallee woody biomass particle sizes due to a sudden contact with steam, this study conducted pyrolysis and gasification experiments by employing two very different biomass particle sizes of 5.18 and 0.14 mm. The structural features of chars were then characterized using FT-Raman spectroscopy. The results indicate that the drastic change in char structure due to contact with steam was largely affected by the particle size of biomass and temperature. A short period of holding in argon at peak temperature exerted very little effect on the subsequent gasification in steam. Meanwhile, the ratio between small and big aromatics in chars in some circumstances reached a maximum value at around 30 seconds of steam contact owing to the partial “opening” of large fused aromatic rings.

6.1 Introduction

Understanding the changes in char structure during gasification is highly demanded as the structural feature of char is very important for the char reactivity [1-5]. However, the characterisation of char structure has always been a challenge due to the special carbon skeleton structural features of chars, which do not contain the well defined graphite crystals [6], but consists mainly of different sizes of fused aromatic rings [6,7]. As XRD would have many shortcomings to characterize char structure, many researchers have attempted the Raman spectroscopy based on the procedures proposed by Tuinstra and Koenig [8-14]. However, this has not been very successful because the procedures was based on the study on graphite [15]. A new approach was developed in our group to characterise the chars obtained from the thermal treatment of coal and biomass at relatively low temperatures (<1000°C) [6]. The broad spectra for all chars could be successfully deconvoluted/curve-fitted with 10 bands representing the typical structures in the chars [1, 3, 4, 6].

Our study has directly and indirectly shown the importance of char structure to reactivity from Victorian brown coal under different experimental conditions [1, 3, 6, 16-21]. A close relationship was revealed between char reactivity and structural features of carbon skeleton, such as the ratio between small (3-5 fused rings) and big (no less than 6 fused rings) aromatic ring systems, the cross linking structure and functional groups. However, little is known about the changes in biomass char structure during gasification, which is essential to realize is efficient use of the renewable energy resource.

Recently, one paper from our group reported that there was a sudden change in char structure when char from the pyrolysis of cane trash biomass contacted with steam for a very short period (20 seconds) [22]. The sudden change in char structure was explained by considering that the H radicals from the gasification reaction have penetrated into the char and activated the growth of aromatic rings. However, the extent of penetration into the bulk structure of char might be limited if the char particle size significantly increases. The importance of biomass particle size to the change in char structure was sighted in previous chapter as shown in Figure 5-3. Therefore, there is a need to explore the possible different behaviours between small and big particles of biomass when they suddenly contact with steam after pyrolysis.

This study aims to examine the alteration in char structure during the gasification of both small and large particle sizes of mallee woody biomass in steam following the pyrolysis at a slow heating rate. Significant changes in char structure were observed upon the contact of char with steam. Particle size was found to be a crucial factor influencing the changes in char structure.

6.2 Results and discussion

6.2.1 Char conversion profile during the gasification in steam

Figure 6-1 shows the char yields as a function of gasification time in steam after the chars were prepared at a slow heating rate of 10 °C/min up to 800 and 700 °C with 0 or 15 min holding. As expected, the higher pyrolysis/gasification temperature of 800 °C resulted in lower char yields than those at 700 °C. For a given set of temperature and gasification time, the char conversion was always the same irrespective of the holding time in argon (0 or 15 min), indicating that the thermal annealing at the peak temperatures had very little effect on char reactivity under the present experimental conditions. The particle size showed a strong effect on char conversion. Part of released volatiles may condense and polymerize on intra char particle surface. The less extent of devolatilisation and the secondary reaction in the large particle have led to the higher char yields shown above [23]. Nevertheless, it seems that the subsequent gasification rates in steam for the two different particle sizes used were very close. This actually doesn’t mean that the changes in char structure during the process followed the same trend, which will be discovered below.

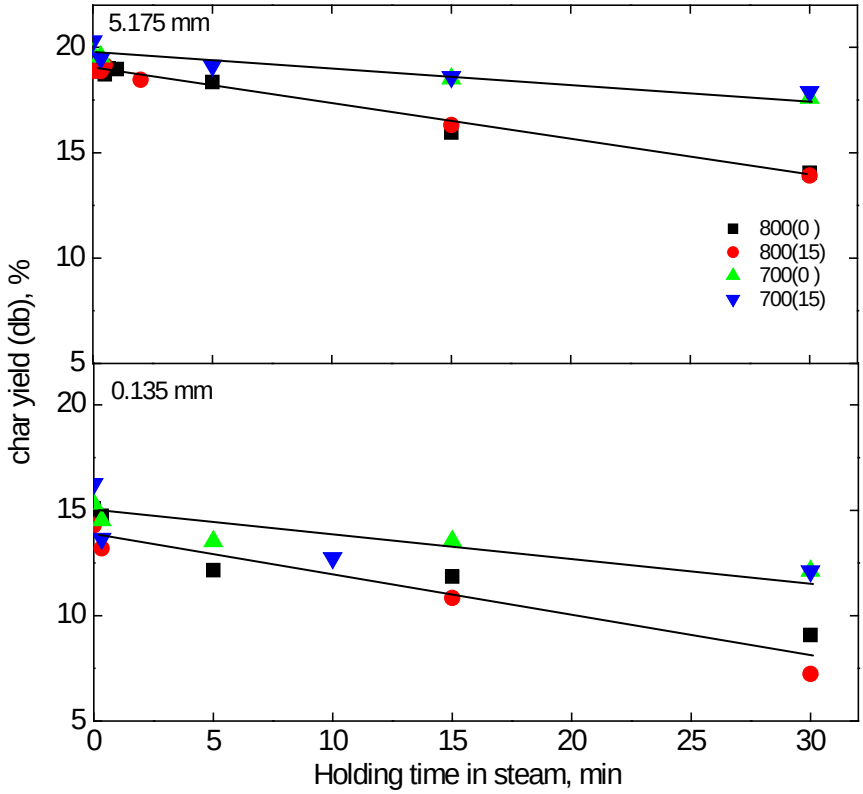

Figure 6-1. Char yields as a function of holding time (gasification time) in steam and temperature after pyrolysis. “800(0)” denotes the initial char that was prepared from the pyrolysis by heating at 10 K/min up to 800 ^{o}C with 0 min holding time in argon prior to the introduction of steam.

6.2.2 Changes in the ratios I_{GR}/I_D and $I_{(GR+VL+VR)}/I_D$ during gasification

It is illustrated in Figure 6-2 that the I_{GR}/I_D band area ratio changed with the gasification time. The G_R band mainly represents small aromatic ring systems (3-5 fused rings) while D band symbolises large aromatic ring systems (not less than 6 fused rings) for the chars from the pyrolysis and gasification of low rank fuels [1, 3, 4, 6]. The trend presented in Figure 6-2 reflects the changes in the ratio between small and large aromatic ring systems in the chars. The thermal annealing at 800 ^oC results in a considerably lower I_{GR}/I_D band area ratios than those of 700 ^oC in Figure 6-2, implying that the aromatisation of char structure took place dramatically when the temperature was increased by 100 ^oC although the solid char was not seen to be further converted into gaseous products (see the starting datum points in Figure 6-1). At the gasification temperature of 700 ^oC, the I_{GR}/I_D ratio for both sizes of samples showed a decreasing trend. The slow decreases were mainly due to the preferential removal of small aromatics, which was supported by the corresponding reduction in char yields in Figure 6-1.

The ratio for the small particles at the gasification temperature of 800 ^oC showed a similar curve to those of 700 ^oC. The I_{GR}/I_D ratio for the small particles at 800 ^oC drastically decreased within 20 seconds of contact with steam, which is consistent with the result reported by Kowen [22]. H radicals derived from the contact with steam were believed to have penetrated into the char bulk structure and initiated the reaction of aromatic ring growth.

However, for the large particles at the gasification temperature of 800 ^{o}C, the I_{GR}/I_{D} ratio sharply increased during the gasification time between 0-30 seconds followed by a sudden and then slow decrease with the further gasification in steam. It appears that the explanation for the structure change in small particles did not work here. The H radicals produced from the reaction between char and steam could still mobilise into char matrix to a great extent. However, the source of H radicals in the char matrix was mainly from the reaction between steam and char in the absence of volatiles. The relative surface area accessible to react with steam in the large particle could be much smaller than that in the small particle. Thus, the active H radicals in the matrix of large particles might not be as concentrated as in the small particles. Therefore, the sparse activated/broken aromatic fragments by the H radicals could not connect each other in time and could be trapped when we quenched the reaction immediately, as it is shown in Figure 6-2. If given longer gasification time, more generated H radicals would penetrate into the char bulk, continue to “open” more fused aromatic rings and enhance the aromatic ring growth. The continued condensation plus the rapid consumption of reactive small aromatics by steam would certainly reduce the ratio I_{GR}/I_{D} at a fast rate.

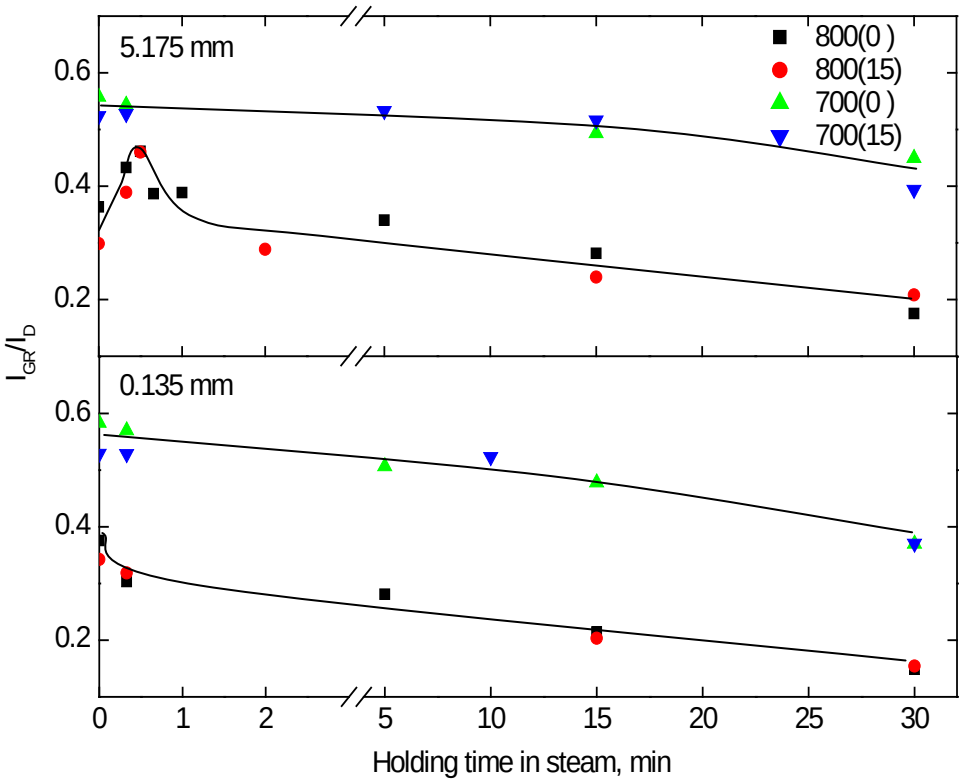

Figure 6-2. G_R to D bands area ratios as a function of time and temperature of steam gasification using different biomass particle size.

The changes of band area ratio between $I_{(GR + VL + VR)}$ and I_D are shown in Figure 6-3. The group of G_R + V_L + V_R bands mainly represents amorphous carbon structure, methylene or methyl group and semi-circle breathing of aromatic rings [6], of which G_R mainly represents small aromatics (3-5 fused rings) discussed above. Furthermore, the band area of V_L and V_R could also be contributed by aliphatics and carboxylates. However considering the temperatures used, the amount of aliphatics and carboxylates in chars would be very limited [22]. Figure 6-3 shows that the value of $I_{(GR + VL + VR)}/I_D$ decreased more significantly over the gasification time although it followed very close trend to that of I_{GR}/I_D in Figure 6-2. In other words, the value $I_{(VL}+_{VR)}$ contributed from methylene or methyl group and semi-circle breathing of aromatic rings also apparently decreased with respect to the reaction time between char and steam, which was consistent with previous research on brown coal and sugarcane/trash [5, 22, 24].

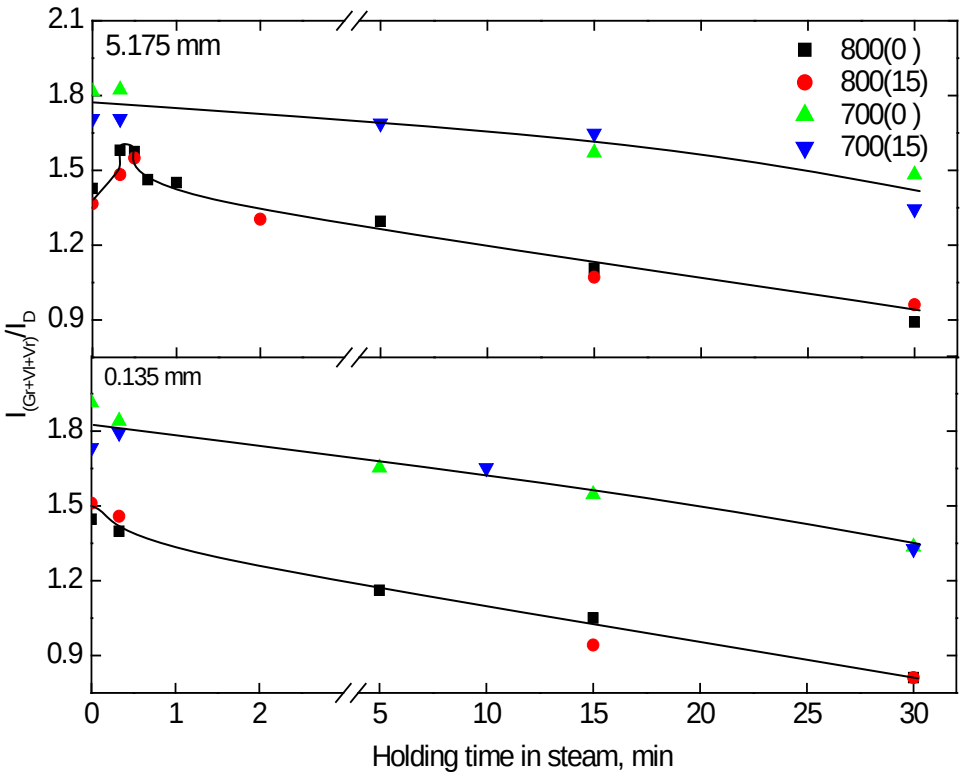

Figure 6-3. Ratios of areas of (G_R + V_L + V_R) to D bands as a function of time and temperature of steam gasification using different biomass particle size.

6.2.3 Changes in total area I_T during gasification

Figure 6-4 presents the total observed Raman peak area between 800 and 1800 cm^{-1} as a function of gasification time in steam for the chars from both large and small particle sizes at the temperatures of 700 and 800 ^oC. Briefly, the total Raman peak area is determined by two structural features of the chars [6, 22]: one is the electron-rich functional groups (i.e. O, S and N containing groups) tending to increase the total Raman area; the other is the aromatization which usually decreases the total Raman area.

The very little effect of particle size could be observed from the comparison between top and bottom parts in Figure 6-4. The apparent difference due to the particle size could be seen only under the experimental condition of 700 ^oC with 15 min holding before the gasification in steam. The large particle led to a higher total Raman area in the early stage (less than 5 min) of gasification time than that for the small particle. As a matter of fact, the higher Raman intensity for the large particle was already formed before the char contacted with steam (i.e. 0 min in Figure 6-4). The I_{GR}/I_D reflecting the relevant abundance of small aromatic ring systems did not really change in Figure 6-2, which meant that the substantial O-containing groups could have thermally cracked and released from the small particle during the 15 min holding in argon. In contrast, the released fragments in large particle may be less significant. The O-containing functional groups may exert resonance effect on aromatic ring systems, thus intensifying the total observed Raman area.

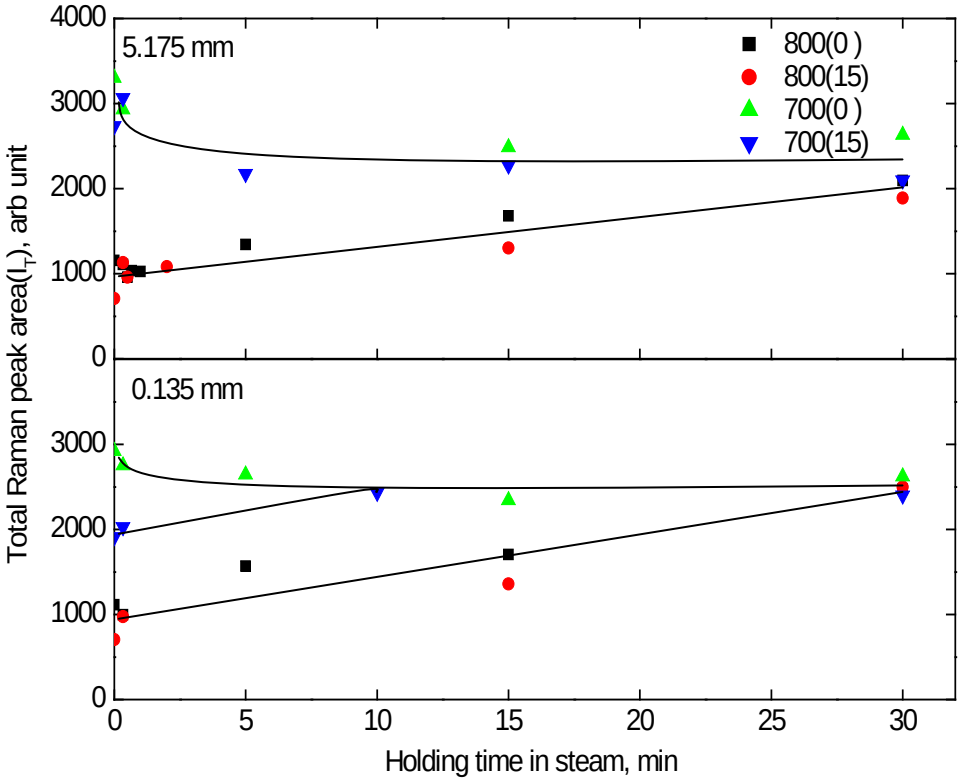

Figure 6-4. Total observed peak area/intensity between 800 and 1800 cm^{-1} as a function of time and temperature of steam gasification.

The impact of temperatures on the total observed Raman area/intensity was very dramatic as shown in Figure 6-4. The total Raman area at 700 ^{o}C decreased during a short period of gasification and then stayed almost constant with increasing gasification time until 30 min while the low intensity for the chars from 800 ^{o}C increased nearly monotonically. Consequently, the differences in the total Raman area between the two temperatures decreased as the gasification time increased.

Clearly, the dramatic decrease in Raman area from 700 to 800 ^{o}C before the introduction of steam (i.e. 0 min) was due to the sever volatilization of those electron-rich functional groups and ring condensation. However, the abandunt polar functional groups (part of amorphous structure) existing in chars at 700 ^{o}C would be released due to the slow gasification and thermal cracking. This should be the main reason for the drop in the Raman area for the chars at 700 ^{o}C. Furthermore, the subsequent weak gasification in steam (shown in Figure 6-1) caused very little change in the total area. On the other hand, gasification at 800 ^{o}C took place significantly and some oxygen component from H_2O could become part of char structure in the form of oxygen complexes, which likely explained the continuous increase in the Raman area.

6.2.4 Changes in the ratio I_S/I_T during gasification

The S band represents $C_{aromatic}$–C_{alkyl}, aromatic (aliphatic) ethers, C–C on hydroaromatic rings, hexagonal diamond carbon sp^3 and C–H on aromatic rings [3,4]. But for the chars investigated, the S band mainly represents alkyl–aryl C–C structures and methyl carbon [3, 4, 6]. Particularly, the S band can be regarded as a crude measurement of cross-link structures in the char. Figure 6-5 shows that the density of S band, as a percentage of the total peak area between 800 and 1800 cm^{-1}, was nearly constant regardless of experimental conditions used in this study. The fact that two different particle sizes of 0.135 to 5.175 mm led to the same relative intensity of S band indicates the negligible effect of secondary reactions on decompositions/formations of the S band-represented sp^3-rich (or sp^3–sp^2 mixture) carbon structure. The percentage of S band did not change with increasing temperature from 700 ^oC to 800 ^oC, suggesting that the cross-link structures were very stable after being treated at 700^oC so that it could not be removed independently. This indicates that the structures represented by the S band were not the sites for preferential consumption in steam gasification.

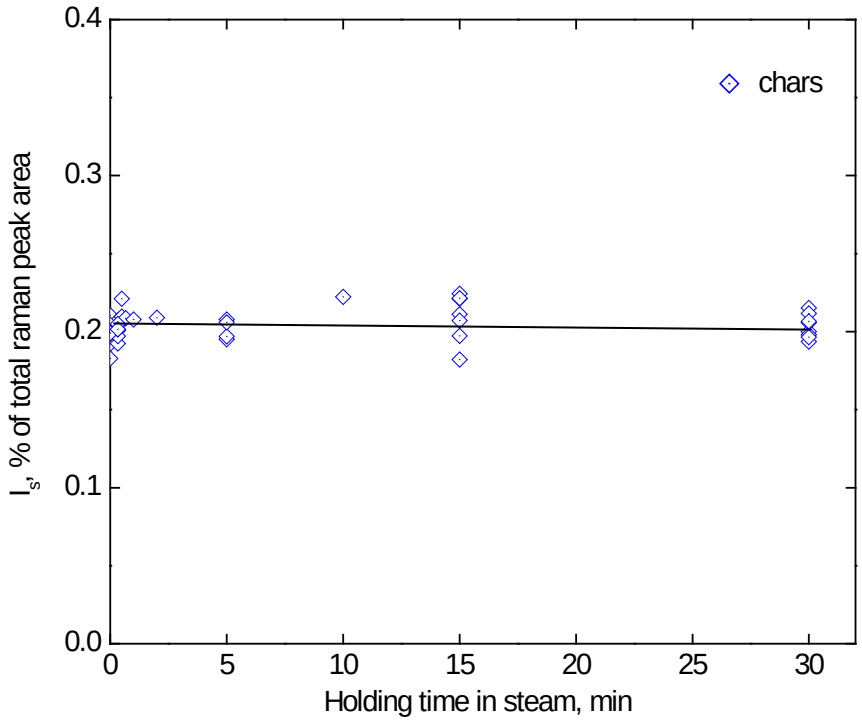

Figure 6-5. I_S/I_T ratio as a function of time and temperature for the chars prepared from both 700 and 800 ^oC using the two particle sizes.

6.3 Conclusions

From the discussion above, conclusions can be made as follows:

- Small aromatics in big biomass particles could be suddenly created in a very short period contact with steam.
- Loss or gain of O-containing functional groups during pyrolyis and gasification was the key for the total observed Raman area/intensity.
- Cross-linking structure (represented by S band) would not be consumed unless the structure unit that it bonded to was removed.

6.4 References

[1] Li C-Z. Fuel 2007;86:1664–1683.

[2] Wu H, Hayashi J-i, Chiba T, Li C-Z. Fuel 2004;83:23–30.

[3] Li X, Hayashi J-I, Li C-Z. Fuel 2006;85:1509–17.

[4] Li X, Li C-Z. Fuel 2006;85:1518–25.

[5] Guo X, Tay HL, Zhang S, Li C.-Z. Energy & Fuels (acceptted).

[6] Li X, Hayashi J-I, Li C-Z. Fuel 2006;85: 1700–1707.

[7] Hayashi J-i, Li C-Z. Structure and properties of Victorian brown coal. In: Li C-Z, editor. Advances in the science of Victorian brown coal. Oxford: Elsevier; 2004. p. 11–84 [chapter 2].

[8] Green P-D,Johnson C A,Thomas K-M. Fuel 1983; 62:1013-1023.

[9] Kelemen S-R, Fang H-L. Energy & Fuels 2001; 15:653-658.

[10] Makovsky L-E, Waldstein P, Edwards W-H. Nature (London), Physical Science 1971;231:154-155.

[11] Johnson C-A, Patrick JW, Thomas K-M. Fuel 1986; 65: 1284-1290.

[12] Cuesta A, Dhamelincourt P, Laureyns J, Martinez-Alonso A, Tascon JMD. Journal of Materials Chemistry 1998;8:2875-2879.

[13] Sekine Y, Ishikawa K, Kikuchi E, Matsukata M. Energy & Fuels 2005;19:326-327.

[14] Mochida I, Korai Y, Fujitsu H,Takeshita K, Komatsubara Y, Koba K, Marsh H. Fuel 1984; 63: 136-139.

[15] Tuinstra F, Koenig JL. J. Chem. Phys. 1970;53:1126-1130.

[16] Li X, Wu H, Hayashi J-I, Li C-Z. Fuel 2004;83: 1273–1279.

[17] Wu H, Li X, Hayashi J-i, Chiba T, Li C-Z. Fuel 2005;84:1221-1228.

[18] Quyn DM, Wu H, Li C-Z. Fuel 2002;81:143-149.

[19] Quyn DM, Wu H, Bhattacharya SP, Li C-Z. Fuel 2002;81:151-158.

[20] Wu H, Quyn DM, Li C-Z. Fuel 2002;81:1033-1039.

[21] Sathe C, Hayashi J-I, Li C-Z, Chiba T. Fuel 2003;82:1491-1497.

[22] Keown D. M, Hayashi J.-I, Li, C.-Z. Fuel 2008;87:1127-1132.

[23] Hosokai S, Kumabe K, Ohshita M, Norinaga K, Hayashi J.-I, Li, C.-Z.Fuel 2008 ;87:2914–2922

[24] Keown D. M, Li X, Hayashi J.-I, Li, C.-Z.Energy & Fuels 2007; 21: 1816-1821.

Chapter 7

Conclusions and recommendations for future work

7.1 Introduction

The purpose of this work was to gain a fundamental understanding on the effects of volatile-char interactions on char structure and reactivity during gasification in steam using Victorian brown coal and mallee woody biomass. The effects of volatile-char interactions on char structure, AAEM volatilisation and char reactivity were systematically investigated.

7.2 Conclusions

7.2.1 Effects of volatile-char interactions on char structure during the gasification of brown coal in steam

Volatile-char interactions greatly enhanced the conversion from small aromatic ring systems into big ones during the gasification in steam because H radicals could penetrate into the aromatic ring systems. The steam gasification selectively removed small aromatic ring systems in the absence of volatile-char interactions, but the selectivity became much less significant when the reactive char structure continuously contacted with H radicals. Additionally, O-containing functional groups from volatiles were very critical for the total observed Raman intensity of chars.

7.2.2 Effects of volatile-char interactions on char-H_2O and char-O_2 reactivities

The volatile-char interactions significantly inhibited char conversion during the gasification in steam at 800 ^{o}C. The change in char structure greatly affected char conversion at the early stage of feeding time, while the

occupation of reactive sites by H radical was the main reason for the low char reactivity at the late stage of feeding time.

The *ex-situ* reactivity of the chars in air at 400 ^{o}C was dominated by char structure when the chars were prepared in the presence of continuous volatile-char interactions. In contrast, the Na catalyst played an important role for the reactivity of chars prepared in the absence of volatile-char interactions for some time following the volatile-char interactions.

7.2.3 Effects of volatile-char interactions (mainly in intra-particle) on char evolution during gasification of mallee woody biomass in steam

Secondary reactions due to volatile-char interactions have caused a low char conversion for the large biomass particles in both slow and fast heating rates. The intra-particle volatile-char interactions greatly reduced AAEM volatilisation at the fast heating rate, but little change in char structure was seen with increasing biomass particle size. The char reactivity depended on catalytic species, being largely affected by the nature of heterogeneous char structure, especially for the chars prepared from the fast heating rate.

7.2.4 Changes in char structure due to sudden contact with steam using different particle sizes of mallee woody biomass

Small aromatics in big char particles could be created in a very short period of contact with steam. Loss/gain of O-containing functional groups during pyrolyis and gasification was the key for the observed total Raman area.

7.3 Recommendations for the future work

- Based on the study of the volatile-char interactions, it is clear that the phenomenon should be extensively examined in a wider range of experimental conditions, such as gasification in CO_2, H_2 and even mixture of the gasifying agents. Moreover, different forms of coal and biomass (H-form, Na-form and so on) should be investigated in order to better understand the mechanism of inhibition on char conversion. In the meantime, it may be very helpful if a technique/meathod could be explored to detect the radicals in-situ during the course of gasification/pyrolysis.
- Due to the importance of volatile-char interactions, the experimental scale needs to be enlarged in order to evaluate the effect of volatile-char interactions more practically using different types of gasifiers.
- Mallee biomass is a renewable and sustainable energy source in Western Australia. Syngas can be produced using clean gasification technology while bio-oil could be generated from pyrolysis process. Ideally, mallee biomass could be used as feedstock without the need of being separated into wood, bark and leave. However, practically they may need to be treated differently due to their different chemical compositions and physical properties. Therefore, research on wood should be also extended to bark and leave.